

BOSTON UNIVERSITY
COLLEGE OF ENGINEERING

Dissertation

**TOOLS FOR INTERFACING, EXTRACTING, AND
ANALYZING NEURAL SIGNALS USING WIDE-FIELD
FLUORESCENCE IMAGING AND OPTOGENETICS IN
AWAKE BEHAVING MICE**

by

MARK E. BUCKLIN

B.S., Columbia University, 2009
M.S., Boston University, 2016

Submitted in partial fulfillment of the
requirements for the degree of
Doctor of Philosophy

2019

© 2019 by
MARK E. BUCKLIN
All rights reserved

Approved by

First Reader

Xue Han, Ph.D.
Associate Professor of Biomedical Engineering

Second Reader

David Boas, Ph.D.
Professor of Biomedical Engineering
Professor of Electrical and Computer Engineering

Third Reader

Ian G. Davison, Ph.D.
Assistant Professor of Biology

Fourth Reader

Jerome C. Mertz, Ph.D.
Professor of Biomedical Engineering
Professor of Electrical and Computer Engineering

Fifth Reader

Kamal Sen, Ph.D.
Associate Professor of Biomedical Engineering

for pickle

Acknowledgements

The support and patience I have received from my committee has gone far beyond what should be expected of anyone. I can't thank you enough.

- Xue Han, Ph.D.
- David Boas, Ph.D.
- Kamal Sen Ph.D.
- Jerome Mertz, Ph.D.
- Ian Davison, Ph.D.
- Vickery Trinkaus-Randall, Ph.D.
- Steven Borkan, M.D.

**TOOLS FOR INTERFACING, EXTRACTING, AND
ANALYZING NEURAL SIGNALS USING WIDE-FIELD
FLUORESCENCE IMAGING AND OPTOGENETICS IN
AWAKE BEHAVING MICE**

MARK E. BUCKLIN

Boston University, College of Engineering, 2019

Major Professor: Xue Han, Ph.D.

Associate Professor of Biomedical Engineering

ABSTRACT

Imaging of multiple cells has rapidly multiplied the rate of data acquisition as well as our knowledge of the complex dynamics within the mammalian brain. The process of data acquisition has been dramatically enhanced with highly affordable, sensitive image sensors enable high-throughput detection of neural activity in intact animals. Genetically encoded calcium sensors deliver a substantial boost in signal strength and in combination with equally critical advances in the size, speed, and sensitivity of image sensors available in scientific cameras enables high-throughput detection of neural activity in behaving animals using traditional wide-field fluorescence microscopy. However, the tremendous increase in data flow presents challenges to processing, analysis, and storage of captured video, and prompts a reexamination of traditional routines used to process data in neuroscience and now demand improvements in both our hardware and software applications for processing, analyzing, and storing captured video. This project demonstrates the ease with which a dependable and affordable wide-field fluorescence imaging system can be assembled and

integrated with behavior control and monitoring system such as found in a typical neuroscience laboratory.

An Open-source MATLAB toolbox is employed to efficiently analyze and visualize large imaging data sets in a manner that is both interactive and fully automated. This software package provides a library of image pre-processing routines optimized for batch-processing of continuous functional fluorescence video, and additionally automates a fast unsupervised ROI detection and signal extraction routine. Further, an extension of this toolbox that uses GPU programming to process streaming video, enabling the identification, segmentation and extraction of neural activity signals on-line is described in which specific algorithms improve signal specificity and image quality at the single cell level in a behaving animal. This project describes the strategic ingredients for transforming a large bulk flow of raw continuous video into proportionally informative images and knowledge.

Preface

I have structured this document to roughly coincide with a chronological account of 6 years spent in a neuro-oriented biomedical engineering lab. My role in the lab was centered around exploratory device design and development, mostly targeting application in neuroscience research, with intended users being neuroscientist colleagues. One of the lab's most remarkable assets is the breadth and diversity of its constituents in terms of their skills and experience, both within and between the engineering/development and the science/medical sides of the lab. All efforts stood to benefit from the close proximity to skilled colleagues, most notably for the complementary guide and provide roles that assisted the development process of new devices and the experiments they were intended for.

My initial experience in optoelectronic device development was as an undergrad at Columbia University where I was advised by Elizabeth Hillman, and developed a device that combined thermography and near-infrared spectroscopy in a portable and inexpensive device intended to provide early detection of adverse neoplastic changes through at-home daily monitoring, particularly targeting use by patients with high-risk for breast cancer. I then went to the Das Lab where I developed macroscopic imaging systems used for intrinsic imaging in the visual cortex of awake primates. As a MD/PhD student, I attempt to maintain a potential to adapt the end-products of each development for clinical applicability. The story presented here is rather unusual in that success precedes failure. The volume of tangible presentable results is greatest toward the beginning stages of the work described here. This unusual inversion is what make this story worth hearing, however. Thank you for taking the

time to read this. I hope that at least the technical information provided herein, if not the procedural insight, is valuable in your current or future endeavors.

Contents

1	Introduction: Background and Literature Review	1
1.1	Optical Imaging of Neural Activity	1
1.2	Procedures for Calcium Imaging	3
1.3	Computer Software Environments for Image Processing	4
1.4	Computational Resources for Processing Large Data Sets	5
1.4.1	Graphics Processing Units for Video Processing	7
2	Neural Interfaces: Fabrication, programming, and assembly	11
2.1	Animal Tracking	11
2.1.1	PD mouse model:	11
2.1.2	Metrics of Behavior	12
2.1.3	Behavior Box	12
2.1.4	IR Touchscreen	13
2.1.5	FrameSynx Toolbox	14
2.1.6	Using Computer Vision to track Position and Orientation . . .	14
2.1.7	Mouse in a Bowl	14
2.1.8	Spherical Treadmill	15
2.1.9	Headplate Holder	16
2.1.10	Motion Sensors	17
2.1.11	Generic USB Computer Mouse with Minimal Linux	17
2.1.12	Navigation Sensor Chip with Arduino	18
2.2	Microscopes	19

2.2.1	Background: Brain Imaging and Microscopy in Neuroscience	19
2.2.2	Cameras for Widefield Microscopy	20
2.2.3	Microscope Construction	21
3	Neural Signals: Computational considerations, interpretation and usage	24
3.1	Image Processing	24
3.1.1	Benchmarking & General Performance	25
3.1.2	Buffered Operations	25
3.1.3	Image Pre-Processing & Motion Correction	26
3.1.4	Sequential Statistics	27
3.1.5	Surface Classification: Peaks, Edges, Curvature	28
3.1.6	Online Cell Segmentation & Tracking	29
3.1.7	Signal Extraction from Subcellular Compartments	30
3.1.8	User Interface for Parameter Tuning	30
3.1.9	Image Processing: Tone mapping and Filtering	30
4	Discussion: the last mile in computing for clinicians, engineers, and research scientists	34
4.1	Primary Goals	34
4.2	State of current methods	36
4.2.1	Signal and Noise in Neural Imaging Data	36
4.3	Exponential Expansion in Data Volume	37
4.3.1	Fields sharing these challenges	37
4.3.2	Technological Opportunities to Expect	38
4.4	Incomplete synthesis of actionable knowledge	38
4.5	Clinical translation potential	39
4.6	Cranial Window	39

4.6.1	“Biomimicry” in visual processing	40
4.6.2	Critical Elements	41
4.6.3	Staging Implant Installation & Tissue Access	43
4.6.4	Design Adaptation	43
4.6.5	Rapid fabrication	44
4.6.6	Future improvements	45
References		47
Curriculum Vitae		77

List of Figures

1.1	Comparison of processor architectures	10
2.1	Behavior-box schematic	13
2.2	Automated animal Tracking for “Mouse in a bowl” type experiments	15
2.3	Automated animal Tracking for “Mouse in a bowl” type experiments: (a-d) video overlay showing tracked points	15
2.4	Spherical treadmill (a) Mouse running on a treadmill equipped with virtual reality; (b) water port; (c) application of the water delivery system	16
2.5	Headplate holder (a) front view; (b) top view; (c) bottom view . . .	16
2.6	Motion sensor installation on a spherical treadmill	18
2.7	Basic configuration for a widefield epifluorescence microscope for in-vivo imaging. This first configuration used a phase contrast lens borrowed from an inverted microscope (not recommended).	21
2.8	Widefield fluorescence microscope (Setup 2)	22
2.9	Widefield fluorescence microscope reconfigured (Setup 3)	23
3.1	Interactive parameter adjustment for homomorphic filter operation (local contrast enhancement)	26
3.2	Motion compensated; comparison of uncompensated and compensated frames overlayed with mean image	27
3.3	Feature generation showing complex-valued moving average of distance of each pixel to bounding box corners (post segmentation)	31

3.4 Feature generation of single motion-compensated frame using complex-valued normalized pointwise mutual information of each pixel with its local neighborhood	32
3.5 Pixel-wise statistics of 128 frames (min, max, mean, standard deviation, skewness, kurtosis)	33
3.6 Normalized differential skewness	33

List of source code

1	Incremental update of the pixel statistics (min, max, and first 4 central moments)	29
---	--	----

List of Abbreviations

ROI	Region of Interest
GECI	Genetically Encoded Calcium Indicator
GFP	Green Fluorescent Protein
GCaMP6	Green Calmodulin Protein 6 (GFP /Calmodulin fusion protein)
CMOS	Complementary Metal Oxide Semiconductor
sCMOS	Scientific Complementary Metal Oxide Semiconductor (image sensor)
PCA	Principal Component Analysis
LINPACK	Linear Algebra Package
BLAS	Basic Linear Algebra Subprograms
GPU	Graphics Processing Unit
CUDA	Compute Unified Device Architecture (NVIDIA GPU programming)
ALU	Arithmetic Logic Unit
POS	Point of Sale
REPL	Read Evaluate Print Loop
SPMD	Single Program Multiple Data
SIMD	Single Instruction Multiple Data
FFT	Finite Fourier Transform
IFFT	Inverse Finite Fourier Transform
PMI	Pointwise Mutual Information
nPMI	Normalized Pointwise Mutual Information
AAV	Adeno-Associated Virus
DVS	Dynamic Vision Sensor
LED	Light Emitting Diode
CAD	Computer-Aided Design
DOG	Difference Of Gaussian (distributions)
FWHM	Full-Width at Half Maximum
LGN	Lateral Geniculate Nucleus
PDF	Probability Distribution Function
\mathbb{R}^2	the Real plane

Chapter 1

Introduction: Background and Literature Review

1.1 Optical Imaging of Neural Activity

Optical techniques for observing neural activity have recently advanced owing to both an evolution of digital imaging technology, and the development of engineered proteins that act as fluorescent indicators of neural activity. Image sensors, like those found in scientific-CMOS (sCMOS) cameras are larger, faster, and more sensitive than prior scientific grade cameras. Meanwhile, the latest generation of Genetically Encoded Calcium Indicators (GECIs), collectively called GCaMP6, report fluctuations in neural activation with extremely high fidelity. This combination of developments enables neuroscientists to open a wider channel to the brain than previously possible using conventional epifluorescence microscopy techniques that enable simultaneous recording from hundreds to thousands of neurons. Expanding the fraction of the observable neurons in an interconnected network could improve understanding of neural coding and provide insight into mechanistic properties of neural disease. Additionally, feeding a large set of neural response information to a machine learning algorithm in a neuro-prosthetic application may provide improved predictive performance even when the exact mechanism of prediction is difficult to discern. However, several major challenges currently antagonize the potential benefits of these new technologies:

1. The increased size of raw data from a single imaging session can easily over-

whelm the computational resources typically used to process similar but smaller sets of data.

2. The accumulation of raw data on disk over multiple imaging sessions quickly exceeds the data-storage capacity of most lab-scale servers, forcing researchers to halt data collection to process and delete, potentially creating a “nightmare scenario”.
3. The experimental design and data analysis procedures familiar to neuroscientists for network activity data for 5 to 10 cells produce highly biased spurious results in the absence of numerous stimulus-response repetitions, i.e., trials. The number of repeated trials sufficient to produce an accurate description of the neural response to any stimulus is on the order of $2N$, where N is the number of neurons being measured.

In the chapters that follow I provide background on the general procedure for offline video processing. I also discuss some of the issues that limit execution of these procedures on a large data-set, and the variety of approaches that I and others have attempted to address this issue. I then introduce the streaming approach that is capable of directly processing video during acquisition and extracting signals, thereby saving relevant signals only while also discarding or compressing the raw video. This approach relies on GPU programming and therefore I also provide background on the application of graphics cards for computationally demanding tasks. Using a graphics card for programming in the MATLAB environment is also discussed.

Capturing wide-field fluorescence images at high spatial and temporal resolution enables us to measure functional dynamic changes in multiple cells within a large interconnected network. Extracting a measure for each cell in a way that preserves spatial and temporal continuity with uniform/unbiased sampling of the observed signal is achievable but several factors complicate procedures intended to accomplish

this task. One class of computer-vision procedure commonly applied to this task is image-segmentation (cell-segmentation in histology applications), a procedure that attempts to represent distinct objects in an image by association of each image pixel with one of any number of abstract objects or with the background. A variety of algorithms exist for efficiently performing this operation on single images. Most methods can be extended to operate in a 3rd dimension, applied to stacks of image frames to enable tracking cells at multiple depths, or equivalently over time.

However, motion induced by physiologic changes and animal movement necessitates the correct alignment of all frames in the sequence. Moreover, the massive fluctuations in signal intensity from individual and spatially overlapping cells often breeds unstable solutions for alignment that radically complicate cell identification routines by disrupting temporal continuity. Implementing a reliable procedure for identifying and tracking the same cells in each frame throughout the sequence thus becomes non-trivial.

1.2 Procedures for Calcium Imaging

The general goal of processing image data from functional fluorescence imaging experiments is to restructure raw image data in a way that maps pixels in each image frame to distinct individual cells or subcellular components, called ‘Regions-Of-Interest’ (ROI). Pixel-intensity values from mapped pixels are often reduced by combination to single dimensional ‘trace’ time-series. These traces indicate the fluorescence intensity of an individual neuron over time, and the collection approximates the distinct activity of all individual neurons in the microscope’s field of view. However, this task is made difficult by motion of the brain throughout the experiment and by the apparent overlap of cells in the single image plane due to limitations of the camera’s 2-dimensional perspective. These issues can be partially mitigated with a few image

pre-processing steps. Most importantly is the alignment of images to correct for motion. These options are described in the Methods & Approaches section below. Most software packages specifically geared toward functional imaging implement either of two basic classes of pixel->cell mapping algorithms. One approach is to use image-segmentation routines for computer vision that seeks to combine adjacent pixels into distinct spatially segregated regions representing objects in the image.

The other common approach is to perform an eigenvalue decomposition on the covariance matrix from a stack of image frames (also called spectral decomposition, or Principal Component Analysis, PCA), resulting in an assembly of basis vectors that define the weighting coefficients for each pixel. Multiplying the basis-vectors (i.e., “components”) with all frames produces a one-dimensional trace for each component. The linear combination is similar to the weighted image-segmentation method in that it assigns fractional coefficients to pixels. However, the procedure for computing the covariance matrix employed by PCA operates on as many pixels as exist in the image, multiplying each with every other pixel that creates a problem with NP^2 complexity, where p is the number of pixels in the image. I mention these issues inherent to PCA not because this project addresses them but because this project was initiated following substantial difficulty attempting to use PCA-based cell sorting methods with large data-sets.

1.3 Computer Software Environments for Image Processing

The widespread usage of MATLAB in neuroscience communities lends potential for greater usability and easier adaptation to software developed in this environment. While software development environments focused on “ease-of-use” traditionally presume crippling sacrifices to computational performance, this assumption is now less accurate.

Standard programs include ImageJ, the built-in routines in MATLAB’s Image Processing Toolbox, Sci-Kits Image for Python, and a remarkable diversity of miscellaneous applications. MATLAB is a commercial software development platform that is geared toward fast production and the prototyping of data processing routines in a high-level programming language. It implements several core libraries (LINPACK, BLAS, etc.) that make multi-threaded operations on matrix type data highly efficient. While MATLAB has traditionally been considered the standard across neuroscience research labs, it is well recognized that its performance was lackluster for “vectorized” routines as compared to applications developed using lower-level languages like FORTRAN, C, and C++. Nevertheless, it remained in common use, and recent releases have added features that can drastically mitigate its poor performance issues, particularly through the development of a “Just-In-Time” compiler that automatically optimizes the deployment of computation accelerator resources for standard MATLAB functions. This feature enables code that performs repeated operations using for-loops or while-loops nearly as fast as equivalent code written in C. Additionally, code can be compiled into executable format using the MATLAB Compiler toolbox, or used to generate equivalent C or C++ code using MATLAB Coder.

1.4 Computational Resources for Processing Large Data Sets

Routines for extracting the activity in each cell from a collection of raw imaging data rely on simultaneous access to many pixels separated over space and time (and consequently, are separated on a disk). For long recording sessions however, the size of the collection of stored image data dramatically grows. This substantial increase in data size easily exceeds the capacity of system memory in the typical workstation computer available to most researchers. Thus, performing the necessary processing performance enhancing routines using standard programs is often unfeasible.

Another popular approach to this challenge is the migration of processing routines to a cluster-based system. In this way, image data can be distributed across many interconnected computer nodes capable of performing all locally restricted image processing procedures in parallel and then passing data to other nodes in the cluster for tasks that rely on comparisons made across time. Access to clusters capable of performing in this way has been historically restricted to researchers in universities or other large organization, and the diversity of cluster types is sizeable, with clusters often having very particular configuration requirements for efficiently implementing data processing jobs. These issues pose difficulty to the use and shared development of software libraries for image processing routines, although the growth of “cloud computing” services such as Amazon’s EC2 and the Google Compute Engine, as well as collaborative computing facilities such as the Massachusetts Green High-Performance Computing Center minimize several of these processing issues. Additionally, efforts to produce a standardized interface for accessing and distributing data and for managing computing resources across diverse computing environments have seen appreciable success. Apache’s release of the open-source cluster computing framework, Hadoop, and a companion data-processing engine called Spark, have encouraged a massive growth in collaborative development projects, and consequently increased the availability of robust shared libraries for data processing in a variety of applications. The Spark API can be accessed using the open-source programming Python or other languages including Java, Scala, or R. The Thunder library, a Spark package released by the Freeman lab and developed in collaboration with a number of other groups at Janelia Farm and elsewhere is specifically geared for image processing of neural imaging data.

Many applications will find that the recent improvements in accessibility and standardization make cluster computing an attractive and worthwhile option for pro-

cessing large sets of reusable data. However, this strategy imposes harsh limitations for a neuroscientist engaged in a project that is continuously generating new data, as the time required to transfer entire imaging data sets across the internet may be prohibitive. Unfortunately, storage capacity on the cloud is also quite finite. The required capacity to store the accumulated output from continuous high throughput devices such as image sensors. This rate imbalance is a central motivating issue in this project and is discussed in detail below.

The generation of sCMOS cameras available at the start of this work capture full-frame resolution video at either 30 fps or 100 fps depending on the data interface between camera and computer (USB3.0 or CameraLink). At 16-bits per pixel and 2048x2048 pixels, the maximum data rate for the USB3.0 camera is 240 MB/s. Imaging sessions typically last 30-minutes or less. Pixels are typically binned down 2x2, and frame rate is often reduced to work within the constraints our laboratory workstations impose on processing speed and storage. However, the effect of doubling resolution on processing time when using the graphics card is virtually negligible. Identifying ROIs online and extracting the traces of neural activity allows us to discard acquired images and instead, only store the relevant pixels for later analysis.

1.4.1 Graphics Processing Units for Video Processing

Graphics Processing Units were traditionally developed for the consumer gaming market. They are optimized for the process that involves translating a continuous stream of information into a two-dimensional image format for transfer to a computer monitor. In the context of gaming, the stream of information received by a GPU describes the state of objects in a dynamic virtual environment and is typically produced by a video game engine. These processors are highly optimized for this task. However, they are equally efficient at performing the same procedure type in reverse, reducing a stream of images to structured streams of information about dynamic objects in

the image. These features render them popular for video processing and computer vision applications.

All GPU architectures consists of a hierarchy of parallel processing elements. NVIDIA’s CUDA architecture refers to the lowest level processing element as “CUDA Cores” and the highest level as “Symmetric Multiprocessors.” Typically, data is distributed across cores and multiprocessors by specifying a layout in C-code using different terminology, “threads” and “blocks.” Blocks are then termed to be organized in a “grid.” Adapting traditional image processing or computer vision algorithms to quickly run on a GPU involves efficiently distributing threads and ideally minimizes communication between blocks.

MATLAB makes processing data using the GPU seemingly trivial by overloading a large number of built in functions. Performance varies however. Writing a kernel-type subfunction is often the fastest way to implement a routine written as if it operates on single (scalar) element only that can be called on all pixels at once or employs all pixel-subscripts used by the function to retrieve the pixel value at a given subscript. The kernel-type function is compiled into a CUDA kernel the first time it’s called, then repeated calls directly contact the kernel with minimal overhead. Calls typically use the `arrayfun()` function.

Data transfers between system memory and graphics memory is often a major bottle-neck. Therefore, this operation is best performed only once. However, once data is available to the GPU, many complex operations can be performed to extract information from the image without exceeding the processing-time limit imposed by the frame-rate of the camera sending the images.

In total, this project employs advances in both software and hardware that facilitate rapid accurate image analysis of living organisms with the ultimate goals of simplifying the acquisition and analysis of neural activity indicators in both normal

and pathological states.

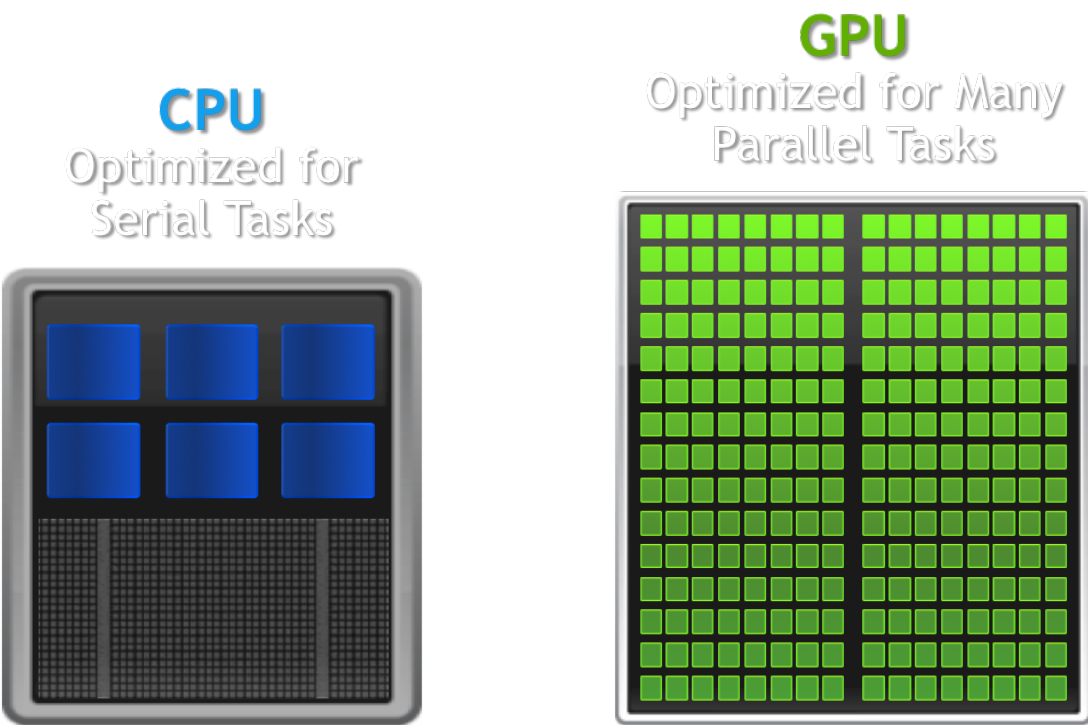


Figure 1·1: Comparison of processor architectures: CPU (left) and GPU (right) differ tremendously in the number of ALUs packed on a chip [<https://www.datascience.com/blog/cpu-gpu-machine-learning>]

Chapter 2

Neural Interfaces: Fabrication, programming, and assembly

This chapter describes several projects that were started early during my graduate studies. Each project is similar in that they are outside the realm of optical imaging of neural activity, which is the focus of the rest of this dissertation. Nevertheless, they are included here because the issues they bring up will later inform the approach I take in the work described in later chapters. The projects described in the following sections are also tied together by a common goal: to enable research in the neurosciences with translation potential for clinical applications.

2.1 Animal Tracking

2.1.1 PD mouse model:

You can induce a quantifiable PD-like state in mice with a unilateral injection of the neurotoxin 6-hydroxydopamine (6-OHDA) into the striatum, and subsequent administration of apomorphine to provoke side-biased motor deficits [Iancu et al., 2005]. Side-biased “turning” behavior is quantified autonomously on two distinct platforms, a computer-vision system that allows free movement, and a virtual-reality spherical treadmill platform that simulates free movement.

2.1.2 Metrics of Behavior

Two testing platforms are used to assess changes in behavior over time. Behavior is analyzed and quantified in real-time, and are synchronized with electrophysiology and made available as stream of events synchronized with imaging and/or electrophysiology. The quantification routine creates a signal that is representative of symptom severity. For our unilaterally lesioned mouse model of PD the most readily observable impairment is the inability to walk straight; mice would turn in circles contralateral to the lesion when given intraperitoneal apomorphine.

2.1.3 Behavior Box

I built an experiment apparatus for mice to enable a study being run by Jia-Min Zhuo. The goal of the study was to elucidate the role of adult-born neurons on mouse behavior, specifically their performance in discrimination tasks. We called the apparatus the “Behavior Box” and modeled it after a commercially available but grossly over-priced box that itself came from other labs (see [McLelland et al., 2015]).

The chamber was constructed with black plastic walls, extruded aluminum framing, and a perforated metal mesh floor 1 cm above a plastic waste tray. A 10-inch infrared touchscreen (ITouch Systems) was mounted over a 10-inch LCD monitor forming one wall of the chamber. An opaque mask with seven windows was placed over the screen to limit where the mouse could touch. A water pump with infrared detector was located at the other end of the chamber to provide reward for the water-deprived mice in the study. A white LED strip encircled the chamber from the top, and multiple speakers positioned outside to deliver sound cues. A web camera was fixed above the chamber to record and monitor mouse activity. My contribution to this project was the program that facilitated interaction between all the system components. This program controlled and recorded experiment progress. I developed the

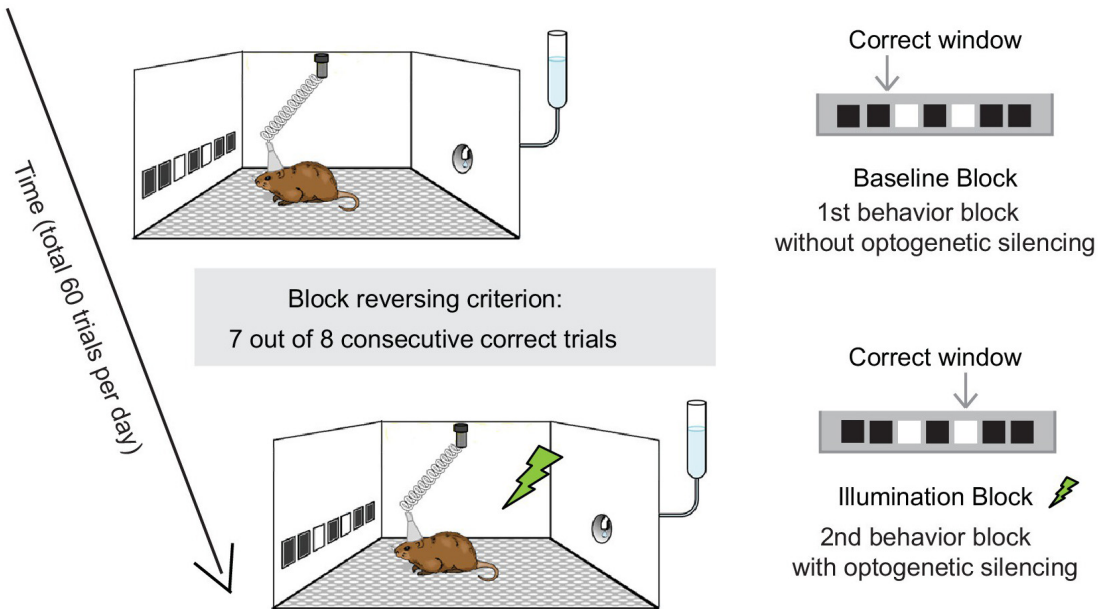


Figure 2.1: Behavior-box schematic

program in MATLAB, and the main components of its function are described below. This system would eventually be used for a study investigating the development of adult-born neurons in the hippocampus [Zhuo et al., 2016].

2.1.4 IR Touchscreen

The IR touchscreen provided a robust measure of the location of any contact with the animal's paws or nose. The screen was more reliable than either *resistive* or *capacitive* touchscreens, which are much more common in devices like POS systems and mobile phones respectively.

The scientists users interact with the device through command-line manipulation of a “BehaviorBox” object in the MATLAB REPL. This approach provides access to features for easily customizable control of physical components including the infrared touchscreen and LCD display along with speakers, water-ports, lights, essentially anything that can be controlled electronically. The approach also enables suggestions

and autocomplete options for users new to the environment.

2.1.5 FrameSynx Toolbox

The FrameSynx toolbox for MATLAB was built to synchronize continuous image acquisition with experiments conducted in the neuroscience laboratory setting. While the experiments are conducted in separate software (and potentially on a different computer), FrameSynx listens for messages to start/stop the experiment, start a trial, etc. and responds accordingly by controlling one or multiple cameras and illumination devices, and synchronizing this information with the data acquired. The major contribution to the “Behavior Box” package, and also to later image processing packages is the procedure for definition and storage and of experimental data files, which will be touched on briefly in chapter 3.

2.1.6 Using Computer Vision to track Position and Orientation

2.1.7 Mouse in a Bowl

A webcam-based motion tracking box constructed to analyze the movement of our unilaterally lesioned PD mouse model. Video is recorded at 15 frames per second and processed on-line or off-line using a function written in MATLAB. Briefly, this function converts each frame to a black and white image (logical matrix), uses morphological filtering functions to isolate the mouse (remove mouse excrement) and identify its body (remove the tail), then finds the center of mass in cartesian coordinates (maximum center of projection on x- and y-axes), and the rostral-caudal orientation measured in degrees off the x-axis. Orientation is determined by the index of maximum of a radon transform of the binary image. Processing is accomplished at a rate of 15-16 fps, using a single core, or 64 fps using parallel processing on a quad-core processor with multi-threading enabled. The advantage of this apparatus over the virtual-reality system is that it allows free movement of an untrained mouse,

with real-time movement metrics at nearly the same rate as the spherical treadmill. This apparatus would go on to be used to investigate the oscillatory dynamics of cholinergic interneurons in the striatum and their association with parkinson's-like motor deficits [Kondabolu et al., 2016].



(a) Raw frame of video being tracked (b) Area of detected mouse (c) Overlay of 3 consecutive frames of mouse between each

Figure 2·2: Automated animal Tracking for “Mouse in a bowl” type experiments

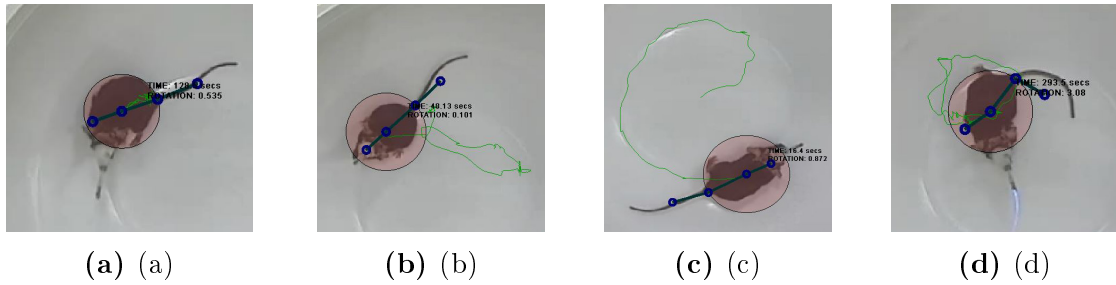


Figure 2·3: Automated animal Tracking for “Mouse in a bowl” type experiments: (a-d) video overlay showing tracked points

2.1.8 Spherical Treadmill

A virtual reality system was assembled, adopting methods from the Harvey lab [Harvey et al., 2009]. This system allows placement of a head-restrained mouse on an 8-inch diameter polystyrene foam ball supported by a cushion of compressed air, surrounded by a toroidal projection screen. Ball rotation is tracked with two optical computer mice placed orthogonal to each other. Movement vectors are fed into a

virtual-reality engine that updates the image projected onto a toroidal screen surrounding the ball, simulating movement through any arbitrary virtual world. Movement vectors are recorded as an arbitrarily scaled translation in the mouse-relative X and Y axes and rotation around the Z axis, at approximately 30 ms intervals. This behavioral apparatus has the advantage of allowing trivial measurement of the mouse's movement ability while the mouse is head-fixed. The disadvantage is the time and potential confounds involved with training individual mice to use the system.

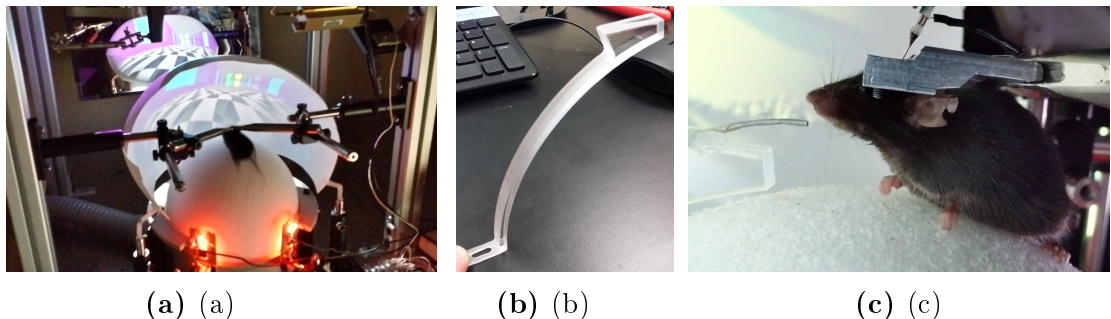


Figure 2·4: Spherical treadmill (a) Mouse running on a treadmill equipped with virtual reality; (b) water port; (c) application of the water delivery system

2.1.9 Headplate Holder

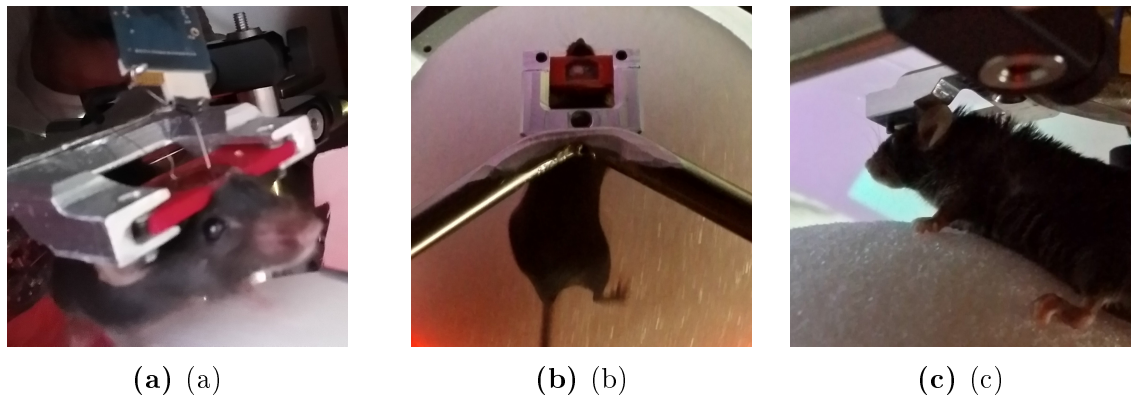


Figure 2·5: Headplate holder (a) front view; (b) top view; (c) bottom view

2.1.10 Motion Sensors

Motion sensing was implemented using a linux computer and standard mice at first, and later using precision laser navigation sensors for “gaming” mice and custom firmware written to work with any arduino-compatible microcontroller.

2.1.11 Generic USB Computer Mouse with Minimal Linux

Run “mouse_relay.py” on any computer running linux to send xy-data from 2 USB optical computer mice to another computer over an RS-232 serial-port connection. The receiving computer (in this implementation) uses MATLAB to read the values and translate the xy-values from 2 mice on the surface of a sphere into 3 values corresponding to rotation of that sphere around 3 orthogonal axes (XYZ) with their origin at the sphere’s center.

RECEIVING FUNCTIONS: The MATLAB class that receives the serial input (xy-values from both mice) is called “VrMovementInterface”

The MATLAB function that translates the double-stream of xy-values from the sphere’s surface into rotation around its center is called “moveBucklin.m” and is located in the VIRMEN “movements” folder.

SERIAL FORMAT: XY-Values are transmitted in ‘packets’ using an ascii formatted string terminated by a newline. Each packet contains the Sensor Number (s) that the reading is coming from, followed by the X-Value (dx), then the Y-Value (dy). The python code looks like the following:

A single reading is received at the other end of the serial connection looking something like the following:

s1x34y-3

2.1.12 Navigation Sensor Chip with Arduino

The system was later improved. I wrote an Arduino compatible library that functions as a driver for the ADNS performance precision gaming sensor. This driver passes $[dx, dy]$ measurements from two ADNS-9800 laser mouse sensors (placed 45-degrees apart on surface of Styrofoam ball). The library has been put to use in multiple systems and enjoys collaborative development from a small number of other researchers [Romano et al., 2019]

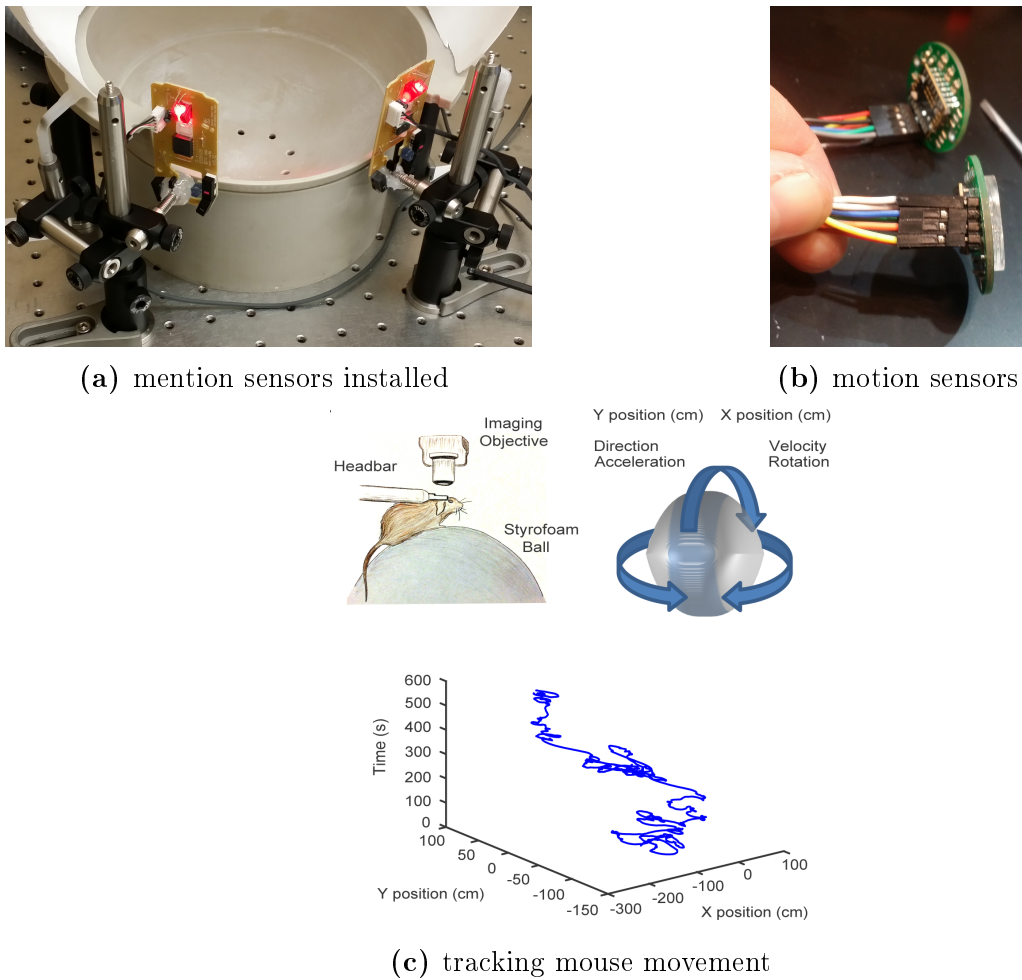


Figure 2-6: Motion sensor installation on a spherical treadmill

2.2 Microscopes

This section describes the background in microscopy in the neurosciences, and also how it relates to imaging in healthcare and electrophysiology in neuroscience. It will also describe the basic elements necessary for the construction of a microscope in a laboratory where calcium imaging in an animal is available. It will also refer to later sections which cover the design and construction of mechanical elements for animal handling and optical access (i.e. the headplate and a chronic optical window).

2.2.1 Background: Brain Imaging and Microscopy in Neuroscience

Optical imaging has traditionally involved wide-field imaging or two photon imaging, each with their own distinctive advantages and disadvantages. In recent years, two photon microscopy has been a preeminent choice for imaging in tissue, because of its high spatial resolution, and tissue penetrating features. Two photon calcium imaging has been broadly applied to individual cells or subcellular components of neurons including spines and axons.

Because two photon microscopy uses a scanning mechanism, the signal to noise ratio is influenced by the time spent imaging each point, and the spatial resolution is determined by the number of points scanned to obtain each image. As a result, the size of the imaging field is inversely correlated with the overall temporal resolution while maintaining a relatively high signal-to-noise ratio, thus, two photon calcium imaging is often performed on a small area or on a sparse network of cells, when dynamic responses with high temporal fidelity is necessary.

Wide-field imaging has been used in various forms for several decades and was first used to characterize the functional architecture and hemodynamic responses in brain tissue. However, this technique has seen a renaissance recently due to its simple instrumentation, relatively inexpensive cost, and the improvements in neural

signal indicators. Optical imaging and two photon microscopy have traditionally been performed in head-fixed preparations, but recent advances have also made it possible to perform wide-field calcium imaging in freely moving animals, through miniaturized and wearable microendoscope systems

While wide-field imaging lacks the spatial resolution to resolve fine subcellular structure or the penetrating properties available with two-photon, it is possible to obtain clear neurites and somatic features, including spike detection

Because a single photon microscope does not rely on scanning features, it can be used to sample a larger field of view without sacrificing sampling rates. Additionally, recording sessions may be less sensitive to fluorophore bleaching than other techniques, which makes it possible to perform sustained illumination and subsequent imaging for an extended period of time - a desired feature for analyzing neural networks during some behavior paradigms (e.g., repeated trial learning paradigms). Thus, wide-field imaging offers an advantage if the objective is to simultaneously recording hundreds of neurons in the brain of a living and behaving animal with high temporal fidelity.

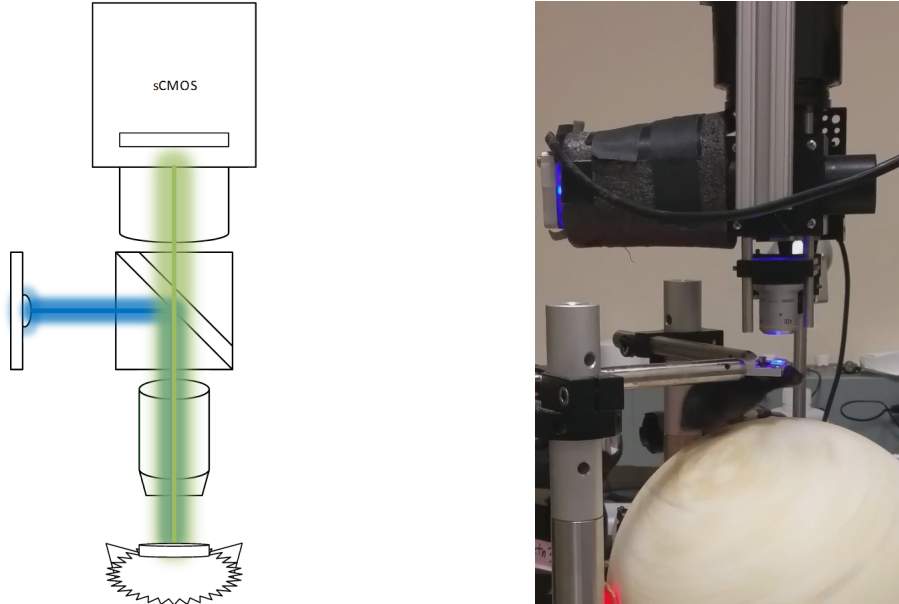
2.2.2 Cameras for Widefield Microscopy

Traditional widefield microscope or macroscope builds incorporate ‘scientific grade’ cameras. Compared to cameras built for other markets – i.e. consumer, industrial, studio, etc. – these cameras are often well tested and certified to offer low or well-characterised noise at moderate speeds, and a linear photo-response profile. Unlike consumer or studio cameras which are invariably configured for RGB color, they are preferably configured with ‘monochrome’ sensors – essentially identical to the analogous color sensor, without the bayer filter. Of much greater importance, one must consider the unique connectivity and control interface that scientific cameras come with. Standards exist, but are typically unique to this segment of the industry,

with poorly defined specifications for translation to other electronic communication and connection interface standards, such as those used in studio and broadcast video, or those used with consumer cameras. The trait that is the most worthy of consideration, however, is the cost.

The in-vivo intrinsic-signal or fluorescent-dye imaging camera of 1 decade ago had a 0.5“-1” monochrome CCD sensor with 0.1-1 MegaPixels, a large well-depth, and moderately low noise at speeds around 30 to 60 fps. Connection was often LVDS, with custom electrical connectors unique to each camera. A particularly popular and long-running model was the Dalsa 1M30, followed by the 1M60 in later years [Takahashi et al., 2006].

2.2.3 Microscope Construction



(a) Schematic showing relation of microscope and mouse on spherical treadmill (b) Setup 1: the LED used for extending to the left (black covering to block light)

Figure 2.7: Basic configuration for a widefield epifluorescence microscope for in-vivo imaging. This first configuration used a phase contrast lens borrowed from an inverted microscope (not recommended).

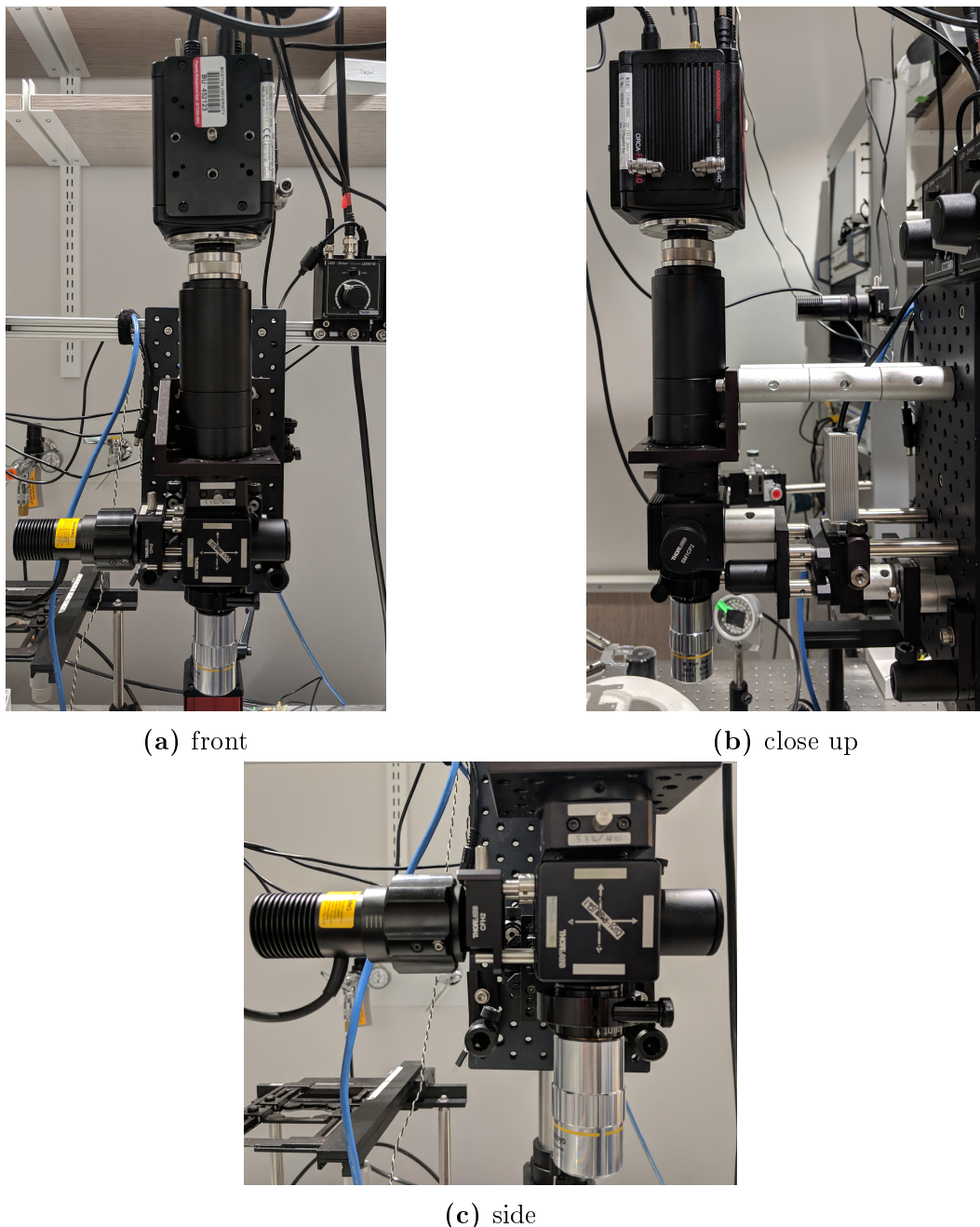


Figure 2·8: Widefield fluorescence microscope (Setup 2)

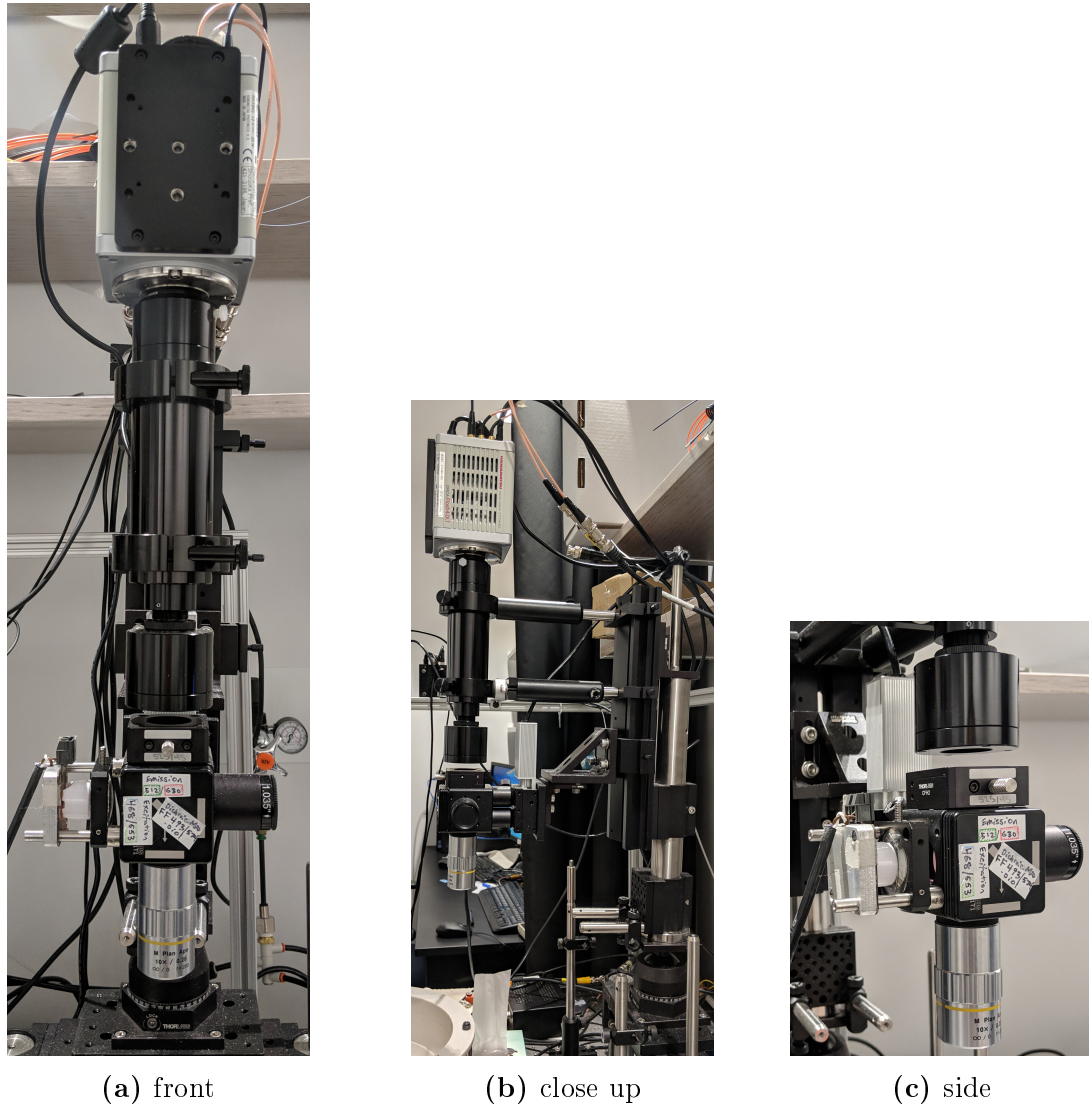


Figure 2·9: Widefield fluorescence microscope reconfigured Setup 3. Multiple iterations are shown, with later iterations offering improved compatibility with usage of off-the-shelf components.

Chapter 3

Neural Signals: Computational considerations, interpretation and usage

3.1 Image Processing

The entire procedure for processing images and extracting cell signals can be performed in substantially less time than most commonly available tools using the approach described in Aim 1, particularly the methods for restricting the spatial extent of pixel-association operations, and distributing operations across parallel processing cores using a Single Program Multiple Data (SPMD) archetype. However, the total time still exceeds that of the acquisition session. Inefficiency arises from the overhead involved with distributing data and passing information between separate parallel processes. Graphics cards, however execute in what's called Single Instruction Multiple Data (SIMD) fashion, to distribute computation across the thousands of processing cores.

The processing components are implemented using the MATLAB System-Object framework, which allows for slightly faster performance through internal optimizations having to do with memory allocation. Most system objects, each representing one step in the serial processing and signal-extraction procedure, also have companion functions that implement the computation-heavy components of each algorithm using a pre-compiled CUDA kernel.

3.1.1 Benchmarking & General Performance

Built-in MATLAB functions that execute on the GPU can be profiled with benchmarking functions like *gputimeit()*, or with the *tic/toc* functions. When execution isn't fast enough, they need to be replaced with custom functions. The custom functions typically achieve the speed up necessary by enabling the operation to be carried out on several frames at once. This reduces the over-head costs imposed for each function call by spreading it over several frames. This solution is not ideal, as it increases the latency of solutions, however does not preclude implementation in real-time system if the procedures are adapted to run on a real-time hybrid system-on-module like NVIDIA's Tegra X1, which should involve minimal effort once a standard set of successful procedures is realized. The current implementation tests the processing time of each stage of the process to ensure that the sum is less than the acquisition time for each frame dictated by the inverse of the frame-rate (30-50 milliseconds).

3.1.2 Buffered Operations

Combining frames for each operation can result in near linear speedup. For example, for the phase-correlation step required for motion correction, the FFT and IFFT are called on 16 image-frames at once, and the time taken to accomplish is approximately the same as if the operation were called on 1 frame. This essentially leads to a 16x speedup, though the latency is also increased slightly. The best size to use is difficult to pre-determine, and typically must be measured for varying size 'chunks' using the benchmarking functions indicated above. The system objects manage the details necessary to allow buffered chunks of video to be passed to each stage without introducing artifacts at the temporal edges between chunks.

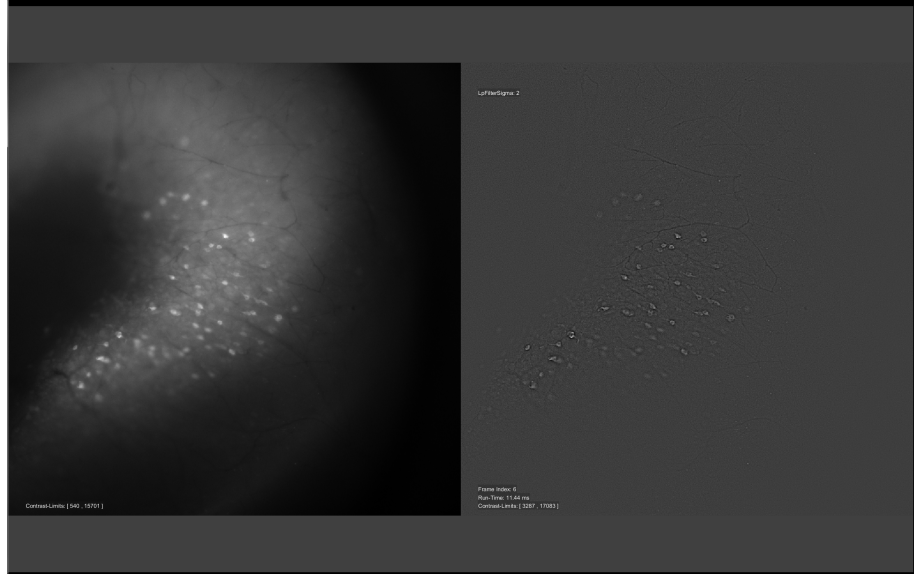


Figure 3.1: Interactive parameter adjustment for homomorphic filter operation (local contrast enhancement)

3.1.3 Image Pre-Processing & Motion Correction

Pre-processing is implemented as with the offline procedure, with a few changes. Images are aligned in chunks, and they are aligned sequentially to two templates. One template is the most recent stable frame from the preceding chunk. The other is a recursively temporal-low-pass filtered image that mitigates slow drifts. Aligning to the first template is usually more stable as the brightness of cells in the recent image will be more similar to those in the current chunk than will be the brightness of cells in the slow-moving average.

The displacement of each frame is found to sub-pixel precision, then used with a custom bicubic resampling kernel that replaces any pixels at the edges with images from the moving average.

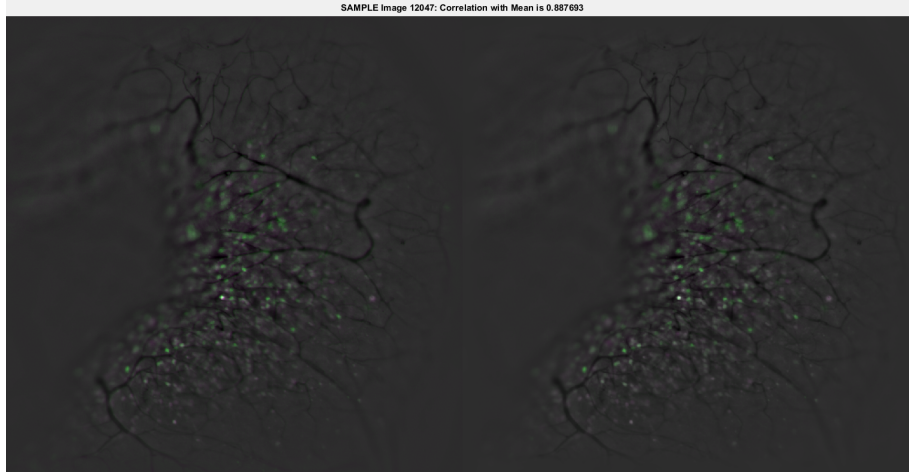


Figure 3-2: Motion compensated; comparison of uncompensated and compensated frames overlayed with mean image

3.1.4 Sequential Statistics

A number of statistics for each pixel are updated online and can be used for normalization and segmentation procedures later in the process. These include the minimum and maximum pixel intensity, and the first four central moments, which are easily converted to the mean, variance, skewness, and kurtosis. The formulas for making these calculations are given below, and are performed in a highly efficient manner as data are kept local to each processing core, and repeat computations are minimized. Code implementing these incremental pixel-wise statistic updates in MATLAB is shown in below 1.

Furthermore, the value used to update each central moment at each point in time can be used as a measure of change in the distribution of each pixel caused by the current pixel intensity, as explained next.

Non-Stationarity & Differential Moments

Stationary refers to the property of a signal such that its statistics do not vary over time, i.e. its distribution is stable. Neural signals tend to specifically *not* have this

property, in contrast to other measurable components such as those contributed by physiologic noise (heart-rate, respirations, etc.) . Thus, by analyzing the evolution of statistical measures calculated for each pixel as frames are added in sequence gives a highly sensitive indicator of neural activity. This is done using a routine analogous to that for updating central moments given above, except the values returned are not only the updated moment, but also the updating component – essentially the partial derivative with respect to time. This is illustrated below, including the normalization functions which convert the partial-moment values to their variance, skewness, and kurtosis analogues:

These functions run on images representing the image intensity, and also on images taken from sequential differences indicating the temporal derivative of image intensity. The combination of outputs from these operations indicate both when image intensities are significantly high relative to past distribution, and also when intensities are changing significantly faster than learned from their past distribution.

This type of function is also easily translated to stencil functions on for computation on the GPU.

3.1.5 Surface Classification: Peaks, Edges, Curvature

Edge-finding methods are employed for establishing boundaries between cells, and first and second-order gradients are used to compute local measures of curvature from an eigenvalue decomposition of the local Hessian matrix. I won't go into detail, as the utility of these procedure in the most recent implementation has been lost, but nevertheless, the operation is optimized and ready to be plugged back in when further development calls for better accuracy informing cell-segmentation, or when a faster or more accurate motion-correction algorithm is called for.

Listing 1 Incremental update of the pixel statistics (min, max, and first 4 central moments). This function can be called to efficiently run in parallel across CPU or GPU cores

```

function [fmin,fmax,m1,m2,m3,m4,n] = statUpdateKernel(f,fmin,fmax,m1,m2,m3,m4,n)

    % update sample count for this pixel
    n = n + 1;

    % precompute & cache some values for speed
    d = f - m1;
    dk = d/n;
    dk2 = dk^2;
    s = d*dk*(n-1);

    % update central moments
    m1 = m1 + dk;
    m4 = m4 + s*dk2*(n.^2-3*n+3) + 6*dk2*m2 - 4*dk*m3;
    m3 = m3 + s*dk*(n-2) - 3*dk*m2;
    m2 = m2 + s;

    % update min & max
    fmin = min(fmin, f);
    fmax = max(fmax, f);

end

```

3.1.6 Online Cell Segmentation & Tracking

Cells are segmented by first running sequential statistics on the properties of identifiable regions on a pixel-wise basis. That is, as regions are identified in a method similar to that used offline in Aim 1, the region-properties are calculated (Centroid, Bounding-Box, etc.) and statistics for these properties are updated at each pixel covered by a proposed region. After sufficient evidence has gathered, Seeds are generated by finding the local peak of a seed-probability function that optimizes each pixel's proximity to a region centroid, and distance from any boundary. Regions are grown from these seed regions, and registered in a hierarchy that allows for co-labeling of cellular and sub-cellular components. Newly identified regions occur as new seeds, where as seeds overlapping with old regions are used to identify sub-regions, or to

track regions over time.

3.1.7 Signal Extraction from Subcellular Compartments

I also have functions for the extraction of normalized Pointwise-Mutual-Information (nPMI), which can operate on a pixel-to-pixel basis or on a region-to-pixel basis. This operation accumulates mutually informative changes in all pixels in the maximal bounding-box (e.g. 64x64 pixels) surrounding each identified regions centroid. The weights given by this function can take on values between -1 and 1, and can be used to inform any reduction operations to follow. Additionally, spatial moments can indicate the subcellular distribution of activity across the identified region. In this context, the first spatial moment M_{00} indicates the mean signal intensity.

3.1.8 User Interface for Parameter Tuning

Some system-objects also incorporate a user interface to aid in parameter selection for tuning.

3.1.9 Image Processing: Tone mapping and Filtering

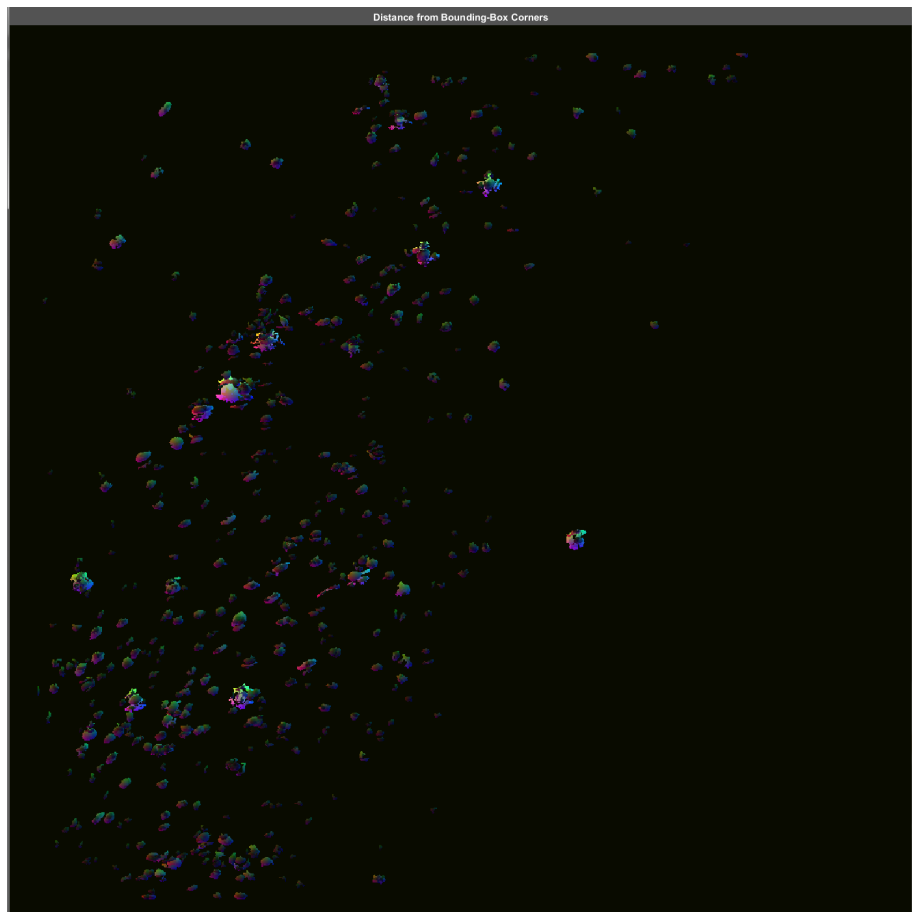


Figure 3·3: Feature generation showing complex-valued moving average of distance of each pixel to bounding box corners (post segmentation)

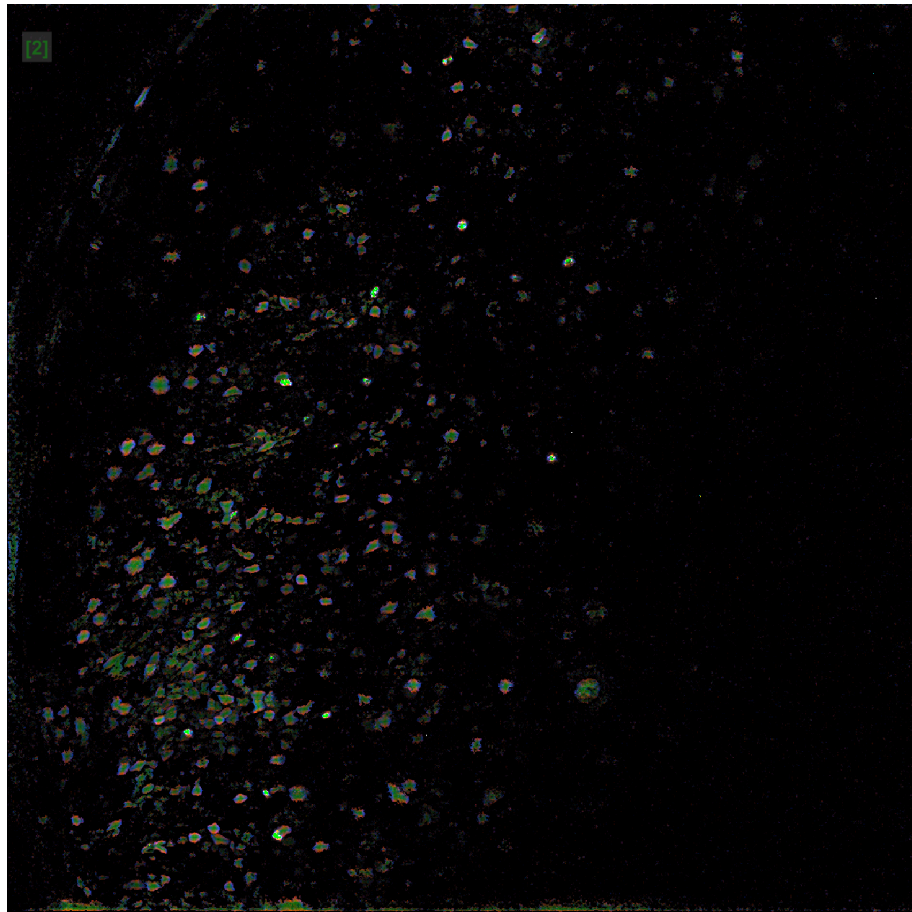


Figure 3·4: Feature generation of single motion-compensated frame using complex-valued normalized pointwise mutual information of each pixel with its local neighborhood

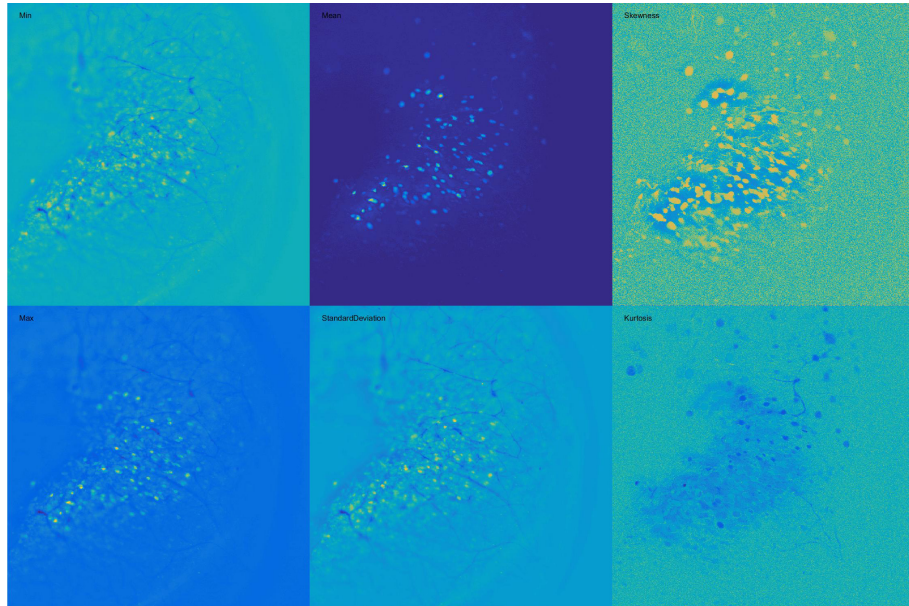


Figure 3·5: Pixel-wise statistics of 128 frames (min, max, mean, standard deviation, skewness, kurtosis)

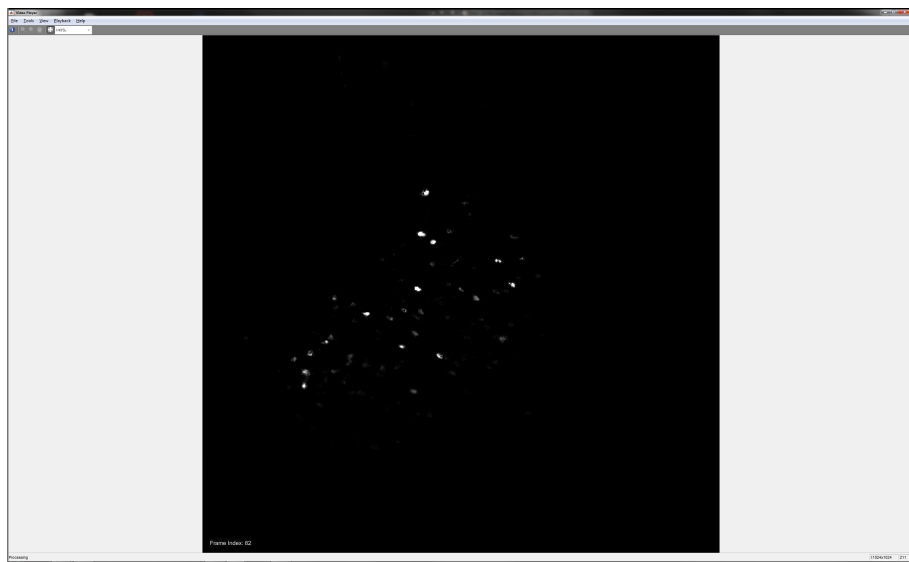


Figure 3·6: Normalized differential skewness

Chapter 4

Discussion: the last mile in computing for clinicians, engineers, and research scientists

This dissertation presents straightforward and reproducible methods for assembling laboratory equipment that can capture the behavior and neural activity of laboratory animals as well as the procedures for managing and analyzing the collected data. In some ways, the recommended procedures deviate from standard practice or the most obvious approaches. In this section, the newer approaches are compared and contrasted with current or traditional ones.

The long-term goal is to improve image quality data analysis in a finite and manageable manner that becomes (perhaps) as elegant, unique, and chaotic as the human brain itself.

4.1 Primary Goals

The function of the brain is to translate/encode sensory input into neural output, actuating an effect that promotes organism survival or the survival of offspring. It achieves this by communicating input through interconnected neurons via converging and diverging connections that comprise the neural network. One way to study the brain is by testing and observing the properties of individual neurons and the response to changing conditions at the direct connections they form with others. Another approach is to observe a collection of neurons and measure their response to variable conditions in their external environment either by recording or stimulating variations

in sensory input or measuring an organism's physical/behavioral response.

One might presume that the expansion of information provided by measuring activity from a larger number of cells in a network would simplify analysis in stimulus-response type experiments and afford insight about underlying functional mechanisms. Unfortunately, the correlation and information theoretic procedures traditionally used to make these associations suffer from a systematic bias that exponentially grows with the number responses considered for each stimulus (i.e., the number of included cells). The trial number necessary to overcome this bias becomes exponentially large although methods such as shuffling/resampling tests exist for bias correction.

A systems neuroscience experiment benefits from online feedback in one or both of two ways:

1. It informs the user regarding the current number of trials, i.e., repeated presentations of the stimulus will be sufficient to overcome limited sampling bias in an experiment attempting to learn the neural response/pattern associated with a specific stimulus. This could be done by testing pattern hypotheses online against subsets of collected data and then assessing their stability.
2. Online pattern recognition feedback maximizes the information in the response to a stimulus either by directing modification of the stimulus, or directing modification of the field-of-view.

Streaming processing addresses the issues of processing and storing pools of data from large networks on the scale that is necessary for deep learning type methods to be effective. Additionally, I demonstrate a strategy in the methods section by which incorporating this online processing stream into stimulus-response-type experiments could help correct limited sampling bias, enabling neural coding analysis in large populations of neurons. This approach works when the experimental intention is to study neural coding in general, for which it's sufficient to have an arbitrary stimulus.

The earliest version of the software mentioned in Chapter 3 was published in 2016 [Mohammed et al., 2016]

4.2 State of current methods

At the start of the work described here, we found ourselves with technology providing “neural signals” that vastly exceeded our expectations and the assumptions of the tools we applied to work with it. In the past, fluctuations in optical imaging data were dominated by “noise.” The form of noise depended on the process; all types of imaging, intrinsic signal, fluorescent dye, etc., had relatively small fluctuations resulting from neural activity. With new engineered molecules, like GCaMP6, and new images sensors, like those dubbed scientific CMOS, these sources of noise were comparatively small. This improved signal-to-noise ratio opens the door for new opportunities and facilitates change to traditional analytic routines. The abundance of signals available from our research animals not only makes old routines inefficient, but paradoxically, also insufficient. Such an abundance of data factors at our finger tips requires a level of discipline in study design to make the scientific method work that was previously unnecessary as the difficulty in finding signals was inherently “self regulating” and inherently limiting.

4.2.1 Signal and Noise in Neural Imaging Data

Traditional noise in neural signals can be roughly categorized as having origin in physiology or technology. The physiological noise sources include “artifacts” caused by an animal’s breathing, heart beat, or other physical movements in response to the experimentally controlled world around them. Technological noise is usually broken down into sensor noise sources: read noise and thermal noise, and noise relating to digitization. A third type of “noise” could arguably be categorized as either, as it lies at the interface of technology and biology. For example, the complex interactions of ex-

ogenous calcium-binding proteins like GCaMP with the endogenous calcium handling proteins of a neuron potentially creates noise at the technology-biology interface. By strict definition, however, only the sensor noise should be termed noise, as other sources are mostly predictable and unpredictable and can be systematically neutralized or accommodated prior to data analysis. The noise level in the signals gathered by a combination of GCaMP6 and a sCMOS camera is minuscule relative to the signals indicating fluctuation in calcium concentration. The problem of visualization of these signals persists however, as the dynamic range of signal varies tremendously over space and time, and requires some treatment prior to being displayed on our currently limited computer monitors. Previously common methods, particularly intrinsic-signal imaging, provided very small signals that required “averaging over time” before any specific or reproducible response could be ascertained.

4.3 Exponential Expansion in Data Volume

The quality of cheaply available image sensors has risen drastically and are readily available. A workable interface can be readily established and the stream of information they provide once switched on is virtually unlimited. In the stark contrast however, storage for this never-ending data stream is both finite in its capacity, and cumulative in its consumption of available storage devices.

4.3.1 Fields sharing these challenges

Scientists often view themselves as working inside laboratory full of sensors, being “data-rich” but “space-poor”. For better or worse, scientists are not alone in dealing with this inherent technological problem. Massive investment has been poured into managing this issue for commercial purposes, and – perhaps unsettlingly – for governmental surveillance purposes. The volume of recordable traffic bouncing through choke points of the internet exceeds the capacity of any government to store for more

than about 24 hours. Likewise, the massive volume of video data acquired by video surveillance systems in China requires a similar solution to one desired by scientists and physicians to resolve our data acquisition challenges.

4.3.2 Technological Opportunities to Expect

Current solutions proposed by commercial and governmental giants are not radical. They include calls for standardization in data format that could enable solutions for efficient transmission and storage to be shared by improving common tools. Common streaming formats allow compression and storage to be abstracted from each application. Databases are being developed to take advantage of heterogeneous computational architectures and distributed storage spaces. Traditional document-based or relational databases are outperformed by graph-based “triple-store” databases, time-series databases, and by databases programmed for specific architecture, including GPU-databases. These technological developments are targeted at the bottlenecks currently restricting access to data. Early results with these approaches suggest an orders of magnitude improvement in throughput. These tools are being developed both with and without the contribution of physicians and scientists. It would be prudent however, to take advantage of new developments by orienting these tools to the specific needs of scientists and clinicians.

4.4 Incomplete synthesis of actionable knowledge

As humans we enjoy dealing in and acting on information with great *certainty*. We have phenomenal acuity for predicting the future, far surpassing that of any other species. Science, the practice of *knowing* has without question accelerated our individual and pan-species capability in this regard, and yet, science deals with surprisingly high levels of *uncertainty*. One might argue that trading, measuring, and learning to affect uncertainty is the general bread and butter of science. Another could say

that, while that is true, the standards for what is a reasonable level of uncertainty are substantially below what they should be.

4.5 Clinical translation potential

Devices that rely on optogenetics to deliver stimulation to neurons inherently share the same hurdles to clinical translation. These hurdles include the requirement for gene-therapy and its associated risks. Several early trials of viral transfection of cells had adverse effects including a greatly increased risk of carcinoma. In these early studies, the DNA insertion location was uncontrolled leaving important regions of DNA tumor suppressor genes exposed to damage. New methods that improve the safety of gene therapy have been developed. Several of the more recent methods utilize adeno-associated virus (AAV) with greater control regarding the site of DNA insertion and also cause less DNA damage. These more recent methods suggest the possibility that with continuing research, methods may be developed without the inherent potential to stimulate malignancy. Working on a project that requires a technology that does not as of yet exist represents one of the greatest educational challenges and benefits of this project. That leap of faith into a future that also does not exist requires us to depend on each other as a team of collaborators in a mutually interdependent manner. In order to succeed, we must do so together. Without each other, our therapeutics would never reach their ultimate “target audience”, the patient. In this scenario, we share both successes and setbacks in the same meaningful way whether such events occur within our own labs or others located elsewhere.

4.6 Cranial Window

The two-stage cranial implant device described here was developed to enable reliable, long-term optical access and intermittent physical access to mouse neocortex. Our

particular application required bilateral cortical windows compatible with wide-field imaging through a fluorescence microscope, and physical access to the underlying tissue for virus-mediated gene delivery and injection of exogenous labeled cells. Optical access is required as soon as possible post-installation and ideally, is sustainable for several months thereafter. My current designs are focused on addressing the issue common to other window designs meant for rodents, that is, progressive degradation of the optical light-path at the brain-to-window interface caused by highly scattering tissue growth. The elastomer insert is molded to fit the chamber and craniotomy site, blocking tissue growth in way that provides a reliable optical interface lasting up to one year. Additionally, the core design can be rapidly adapted to improve its performance or interface with diverse applications.

4.6.1 “Biomimicry” in visual processing

This section describes how computer image and video processing relate to visual processing in the mammalian brain. The overall goal is to emphasize the advantage and importance of bio-mimetic development. Neuromorphic computing with “on chip” image processing represents an improvement over “edge computing”. Event-based image sensors such as the “artificial retina” or DVS attempt to replicate physiologic environments wherein event streams are demanded that are asynchronous and threshold-based. Convolutional neural-nets and deep learning for specific tasks have Genetic programming approaches to procedure optimization will hopefully minimize latency while maximizing sensitivity and accuracy at minimal computational cost, energy expenditure (i.e., with high metabolic efficiency) that facilitates visual stream processing amenable to feature extraction with motion estimation and compensation. The current asymmetry of learning/training time negatively impacts on the desired inference computation time. Common standards applied across projects with common themes can be facilitated by employing rigorous adherence to non-proprietary open

source conventions that includes (but is not limited to) optical parts (lens threads), file formats, widely available software libraries in standard programming languages, and ease of file transmission that are web-based. We are well advised to borrow from related sectors with better developed solutions such as surveillance, media streaming for web/entertainment, sports, astronomy/telescopes, medical imaging and even automotive applications.

4.6.2 Critical Elements

In assessing the design presented here, we highlight a few critical elements that facilitate the maintenance of the long-term optical quality. The Methods section describes the specifics of surgical procedures for head-plate installation and insert attachment. These procedures were established after testing the variable formulations in protocol. First, the design of the silicone insert must incorporate a mechanical barrier that fits along the edges of the craniotomy. To be effective, the barrier must be continuous along the circumference, and extend as far as the inside surface of the skull. Achieving this tight fit without aggressively impinging on the brain requires some sort of fine height adjustment capability. The silicone insert must be attached at the correct height during the installation procedure, or shortly thereafter. The insert must be slightly depressed until full contact is made across the entire window. However, pressing beyond this distance quickly exerts an untoward increase in intracranial pressure that promotes both inflammation and adverse outcomes. A mechanism for fine adjustment can be designed into the system and is in fact incorporated into the installation procedure as is done in the first design and demonstrated in the second design presented here. Of particular note, we found that administration of antibiotic and anti-inflammatory drugs in the days surrounding any major surgical procedure had a substantial impact on the viability of the optical interface. We used both corticosteroid and non-steroidal anti-inflammatory drugs. Attempts to exclude either

drug caused poor outcomes for study animals. Lastly, sealing the chamber is absolutely critical for achieving viability of the optical interface as well as the animal's overall well being. Equally critical to the long-term health of the imaging chamber is the requirement to establish and maintain an air-tight seal between the chamber and the outside world. This includes a permanent seal between the chamber and skull and a reversible seal between the chamber rim and the optical insert. Although specific to the system design, a permanent seal is absolutely essential to ensure long-term functionality. In addition to establishing and maintaining an air-tight seal, it is necessary to eliminate all air pockets within the chamber. Residual air pockets will be susceptible to bacteria growth and may disrupt normal intracranial and intermembrane pressures after installation. We employed sterile agarose fill to displace all air within the chamber prior to sealing. Dead space surrounding the silicone insert, including that temporarily filled with agarose, will fill with fluid and eventually be overtaken by granulation tissue. This preventive process is helpful to the maintenance of a sterile chamber environment and therefore, care should be taken not to disrupt it. However, an excess of dead space will delay this process and thus should also be minimized when adapting the design. Several attempts to test variations from the described procedures indicated that all elements mentioned above are equally critical to achieving a reliable imaging window with sustained optical quality. Implementing the procedures as described or an effective alternative solution should mitigate the primary obstacle to long-term imaging in mice and other rodents by reducing the need to pre-terminate imaging experiments due to light-path disruption by tissue ingrowth. This capability will drastically reduce wasted time and resources for experiments of any duration and facilitate previously infeasible research that require longer-term observations including aging or progressive chronic neurological disorders.

4.6.3 Staging Implant Installation & Tissue Access

Configuring the implant as described to enable a staged installation of multiple parts enables surgical procedures to be easily spread across multiple days. This capability offers a number of advantages including saving time and resources, particularly during the prototype stages by allowing time to ensure each implanted animal fully recovers from the initial procedure and anesthesia. Additionally, the delay between surgeries allows the initial inflammation and immune system responses triggered by craniotomy to resolve before attempting a second intervention in tissue that is sensitive to these manipulations (e.g., viral or cell injections). Importantly, this system affords the capability to image the first tissue intervention from day 0. Similarly, designing a system installed in multiple stages enables trivial and repeatable tissue access at later time points by simply reversing the insert attachment procedure. The process may be comparable to a previously reported method of removing the entire cranial glass window to access the tissue. With this newer system however, the methods used to detach and reattach the cranial window are relatively faster, simpler and carry less risk of tissue damage. Additionally, the described method provide full cranial access without compromising the image field, an advantage not provided by a fixed access port.

4.6.4 Design Adaptation

The specific designs described in this report work well and have much to offer. The potential for fast and unrestricted adaptation is the greatest asset of the underlying system. Most users will find greater utility in adopting components of the design and fabrication process that can be readily customized to fit their exact needs. The design can also be rapidly transformed to accommodate various applications or to modify its performance in response to new technologies and demands. This rapid adaptability

was a primary goal of this project, and informed our design and engineering decisions throughout development. Anyone with access to common laboratory equipment and moderate engineering and fabrication skills can produce a system to fit their particular needs. As an inherent aspect of any design process, the adaptation of the original design evolved over the course of prototyping and testing. In presenting two designs in this report, our intention was to demonstrate the technical feasibility of continuous development of a “future-proof” system. The original system was adapted to accommodate the continuous evolution of image sensor technology, particularly the growth in size and resolution, expanding the field of view and allowing simultaneous access to cellular interactions across multiple brain regions using wide-field imaging. We found that subtle dimensional changes, and the addition of minuscule features exert a large impact on the success of any design. We also found that adjusting features to address one aspect of functionality may have unintended effects. For example, the inclusion of a thin skirt extending below the optical insert that was incorporated to protect against tissue growth within the image field also promotes physical conformity of the brain to the optical window interface over time. This conformity results in a flat imaging plane that is optimal for wide-field imaging and was previously unachievable.

4.6.5 Rapid fabrication

The rapid iterative process used here was made possible by using a combination of widely available rapid prototyping procedures, 3D-printing and laser-cutting. Major progress of manufacturing and its increased versatility, providing better quality, customization, lower cost and shorter production time. In an effort to compare various manufacturing technologies, we explored a number of companies and advanced with 3D metal printing. The final products provided by at i.materialise achieved our experimental goals in product design. We also developed parts in collaboration with other rapid prototyping companies including Shapeways and Sculpteo. In addition:

- Various features and functions of the silicone insert were transformed and extended to conform to new design requirements, some requiring distinctively different design approaches
- Versatility of silicone elastomer to cover a spectrum of design strategies to optimize its configuration might be beneficial
- The design principles that evolved from the initial development are robust and can be applied to new developments or refinements while preserving the successful qualities of the original implant
- CAD designs of these reported systems are open source accessible and can be modified and extended by evolving demands and technologies We, the authors, also call for replication, adaptation, and evaluation (i.e., continued open/shared development).

4.6.6 Future improvements

The current project primarily explores the ability to mold precise and complex features using silicone elastomer to discover configurations to improve image performance using encapsulated electrodes and optical guides. These approaches replace combination optical + integrated electrode window and do not require optogenetics stimulation. More significantly, the encapsulation of carbon, metal colloidal particles or quantum dots into polymer hydrogel networks imparts exclusive thermal, sonic, optical, electrical or magnetic properties. Specifically, the polymer interface may provides a means for directly penetrating neurons to gain electrophysiological recording or facilitate drug infusions, allowing recording and/or manipulation during imaging session. In the near future, improvements in window thickness and chromatic aberration will enhance both wider-field and 2-photon imaging, a process that will be enhanced by improved lenses and embedded, integrated electronic components,

such as LEDs for illumination or stimulation, or sensors. These embedded devices will facilitate positioning, especially in combination with kinematic head-plates that allow for repeatable head positioning and newer fabrication materials.

References

- [Abaya et al., 2012] Abaya, T. V. F., Diwekar, M., Blair, S., Tathireddy, P., Rieth, L., Clark, G. A., and Solzbacher, F. (2012). Characterization of a 3D optrode array for infrared neural stimulation.
- [Abbott and Dayan, 1999] Abbott, L. F. and Dayan, P. (1999). The effect of correlated variability on the accuracy of a population code. *Neural Comput.*, 11(1):91–101.
- [Adapters and Sensor, 1948] Adapters, O. and Sensor, T. (1948). Astronomical instruments. *Nature*, 162:176.
- [Ahrens et al., 2013] Ahrens, M. B., Orger, M. B., Robson, D. N., Li, J. M., and Keller, P. J. (2013). Whole-brain functional imaging at cellular resolution using light-sheet microscopy. *Nat. Methods*, 10(5):413–420.
- [Akidau, 2016] Akidau, T. (2016). The world beyond batch : Streaming 101.
- [Amat et al., 2014] Amat, F., Lemon, W., Mossing, D. P., McDole, K., Wan, Y., Branson, K., Myers, E. W., and Keller, P. J. (2014). Fast, accurate reconstruction of cell lineages from large-scale fluorescence microscopy data. *Nat. Methods*, 11(9):951–958.
- [Andrews, 2010] Andrews, R. J. (2010). Neuromodulation: Advances in the next five years. *Ann. N. Y. Acad. Sci.*, 1199(1):204–211.
- [Asaad and Eskandar, 2008a] Asaad, W. F. and Eskandar, E. N. (2008a). A flexible software tool for temporally-precise behavioral control in Matlab. *J. Neurosci. Methods*, 174(2):245–258.
- [Asaad and Eskandar, 2008b] Asaad, W. F. and Eskandar, E. N. (2008b). Achieving behavioral control with millisecond resolution in a high-level programming environment. *J. Neurosci. Methods*, 173(2):235–240.
- [Asif et al., 2015] Asif, M. S., Ayremlou, A., Sankaranarayanan, A., Veeraraghavan, A., and Baraniuk, R. (2015). FlatCam: Thin, Bare-Sensor Cameras using Coded Aperture and Computation.
- [Barr et al., 2011] Barr, A. M., Boyda, H. N., and Procyshyn, R. M. (2011). Withdrawal. In Olmstead, M. C., editor, *Anim. Model. Drug Addict.*, number 53 in Neuromethods, pages 431–459. Humana Press.

- [Batchelor, 2012] Batchelor, B. G. (2012). Lighting-viewing methods. In *Mach. Vis. Handb.*, pages 319–327. Springer London.
- [Baxter et al., 2008] Baxter, R., Hastings, N., Law, a., and Glass, E. J. (2008). [No Title].
- [Bayati et al., 2015] Bayati, M., Valizadeh, A., Abbassian, A., and Cheng, S. (2015). Self-organization of synchronous activity propagation in neuronal networks driven by local excitation. *Front. Comput. Neurosci.*, 9:69.
- [Beenakker and Schonberger, 2006] Beenakker, C. W. J. and Schonberger, C. (2006). Quantum Shot Noise.
- [Bériault et al., 2012a] Bériault, S., Subaie, F. A., Collins, D. L., Sadikot, A. F., and Pike, G. B. (2012a). A multi-modal approach to computer-assisted deep brain stimulation trajectory planning. *Int. J. Comput. Assist. Radiol. Surg.*, 7(5):687–704.
- [Bériault et al., 2012b] Bériault, S., Subaie, F. A., Collins, D. L., Sadikot, A. F., and Pike, G. B. (2012b). A multi-modal approach to computer-assisted deep brain stimulation trajectory planning. *Int. J. Comput. Assist. Radiol. Surg.*, 7(5):687–704.
- [Berlin et al., 2015] Berlin, S., Carroll, E. C., Newman, Z. L., Okada, H. O., Quinn, C. M., Kallman, B., Rockwell, N. C., Martin, S. S., Lagarias, J. C., and Isacoff, E. Y. (2015). Photoactivatable genetically encoded calcium indicators for targeted neuronal imaging. *Nat. Methods*, 12(9):852–858.
- [Bernstein et al., 2012] Bernstein, J. G., Garrity, P. A., and Boyden, E. S. (2012). Optogenetics and thermogenetics: Technologies for controlling the activity of targeted cells within intact neural circuits. *Curr. Opin. Neurobiol.*, 22(1):61–71.
- [Bertschinger et al., 2014] Bertschinger, N., Rauh, J., Olbrich, E., Jost, J., and Ay, N. (2014). Quantifying unique information. *Entropy*, 16(4):2161–2183.
- [Bessell, 1990] Bessell, M. S. (1990). UVBRI bandpass. *Publ. Astron. Soc. Pacific*, 102(October):1181–1199.
- [Betelak et al., 2001] Betelak, K. F., Margiotti, E. A., Wohlford, M. E., and Suzuki, D. A. (2001). The use of titanium implants and prosthodontic techniques in the preparation of non-human primates for long-term neuronal recording studies. *J. Neurosci. Methods*, 112(1):9–20.
- [Bevilacqua et al., 1999] Bevilacqua, F., Piguet, D., Marquet, P., Gross, J. D., Tromberg, B. J., and Depeursinge, C. (1999). In vivo local determination of tissue optical properties: applications to human brain. *Appl. Opt.*, 38(22):4939.

- [Blanchard and Greenaway, 2000] Blanchard, P. M. and Greenaway, A. H. (2000). Broadband simultaneous multiplane imaging. *Opt. Commun.*, 183(1):29–36.
- [Bonissone et al., 2011] Bonissone, P. P., Xue, F., and Subbu, R. (2011). Fast meta-models for local fusion of multiple predictive models. *Appl. Soft Comput. J.*, 11(2):1529–1539.
- [Bonnet et al., 2001] Bonnet, P., Gehrke, J., and Seshadri, P. (2001). Towards Sensor Database Systems.
- [Boominathan et al., 2014] Boominathan, V., Mitra, K., and Veeraraghavan, A. (2014). Improving resolution and depth-of-field of light field cameras using a hybrid imaging system.
- [Bosl et al., 2013] Bosl, W., Mandel, J., Jonikas, M., Ramoni, R. B., Kohane, I. S., and Mandl, K. D. (2013). Scalable decision support at the point of care: A substitutable electronic health record app for monitoring medication adherence. *J. Med. Internet Res.*, 15:e13.
- [Bosse et al., 2015] Bosse, J. B., Tanneti, N. S., Hogue, I. B., and Enquist, L. W. (2015). Open LED illuminator: A simple and inexpensive LED illuminator for fast multicolor particle tracking in neurons. *PLoS One*, 10:1–21.
- [Botcherby et al., 2008] Botcherby, E. J., Juškaitis, R., Booth, M. J., and Wilson, T. (2008). An optical technique for remote focusing in microscopy. *Opt. Commun.*, 281(4):880–887.
- [Bria et al., 2016] Bria, A., Iannello, G., Onofri, L., and Peng, H. (2016). TeraFly: real-time three-dimensional visualization and annotation of terabytes of multidimensional volumetric images. *Nat. Methods*, 13(3):192–194.
- [Bridgeford et al., 1980] Bridgeford, P. H., Lowenstein, M., Bocanegra, T. S., Vasey, F. B., Germain, B. F., and Espinoza, L. R. (1980). Polymyalgia rheumatica and giant cell arteritis: Histocompatibility typing and hepatitis-B infection studies. *Arthritis Rheum.*, 23(4):516–518.
- [Brown et al., 2012] Brown, D. A., Kim, J. H., Lee, H. B., Fotouhi, G., Lee, K. H., Liu, W. K., and Chung, J. H. (2012). Electric field guided assembly of one-dimensional nanostructures for high performance sensors. *Sensors (Switzerland)*, 12(5):5725–5751.
- [Broxton et al., 2013] Broxton, M., Grosenick, L., Yang, S., Cohen, N., Andelman, A., Deisseroth, K., and Levoy, M. (2013). Wave optics theory and 3-D deconvolution for the light field microscope. *Opt. Express*, 21:25418.

- [Bumstead and Moran, 2017] Bumstead, J. R. and Moran, D. (2017). Multiscale imaging of the mouse cortex using two- photon microscopy and wide-field illumination. *Eng. Appl. Sci. Theses Diss.*
- [Campagnola et al., 2014] Campagnola, L., Kratz, M. B., and Manis, P. B. (2014). ACQ4: an open-source software platform for data acquisition and analysis in neurophysiology research. *Front. Neuroinform.*, 8:3.
- [Campana and Keogh, 2010] Campana, B. J. and Keogh, E. J. (2010). A compression-based distance measure for texture. *Stat. Anal. Data Min.*, 3(6):381–398.
- [Carignan and Yagi, 2012] Carignan, C. S. and Yagi, Y. (2012). Optical endomicroscopy and the road to real-time, *in vivo* pathology: present and future. *Diagn. Pathol.*, 7(1):98.
- [Carro et al., 2015] Carro, A., Perez-Martinez, M., Soriano, J., Pisano, D. G., and Megias, D. (2015). IMSRC: Converting a standard automated microscope into an intelligent screening platform. *Sci. Rep.*, 5:10502.
- [Chacron et al., 2003] Chacron, M. J., Longtin, A., and Maler, L. (2003). The effects of spontaneous activity, background noise, and the stimulus ensemble on information transfer in neurons. *Netw. Comput. Neural Syst.*, 14(4):803–824.
- [Chan et al., 2009] Chan, D. T., Zhu, X. L., Yeung, J. H., Mok, V. C., Wong, E., Lau, C., Wong, R., Lau, C., and Poon, W. S. (2009). Complications of deep brain stimulation: A collective review. *Asian J. Surg.*, 32(4):258–263.
- [Chan et al., 2015] Chan, L. W. C., Pang, B., Shyu, C.-R., Chan, T., and Khong, P.-L. (2015). Genetic algorithm supported by graphical processing unit improves the exploration of effective connectivity in functional brain imaging. *Front. Comput. Neurosci.*, 9:50.
- [Chan et al., 1982] Chan, T. F., Golub, G. H., and LeVeque, R. J. (1982). Updating Formulae and a Pairwise Algorithm for Computing Sample Variances. In *COMPSTAT 1982 5th Symp. held Toulouse 1982*, pages 30–41. Physica-Verlag HD.
- [Chan et al., 1983] Chan, T. F., Golub, G. H., and Leveque, R. J. (1983). Statistical computing: Algorithms for computing the sample variance: Analysis and recommendations. *Am. Stat.*, 37(3):242–247.
- [Chawla, 2016] Chawla, D. S. (2016). The unsung heroes of scientific software. *Nature*, 529(7584):115–116.

- [Chen et al., 2013] Chen, B. T., Yau, H. J., Hatch, C., Kusumoto-Yoshida, I., Cho, S. L., Hopf, F. W., and Bonci, A. (2013). Rescuing cocaine-induced prefrontal cortex hypoactivity prevents compulsive cocaine seeking.
- [Chen and Harrison, 2002] Chen, J. and Harrison, D. E. (2002). Quantitative trait loci regulating relative lymphocyte proportions in mouse peripheral blood. *Blood*, 99(2):561–566.
- [Chen et al., 2017] Chen, R., Canales, A., and Anikeeva, P. (2017). Neural recording and modulation technologies. *Nat. Rev. Mater.*, 2(2):1–16.
- [Chien et al., 2017] Chien, M.-P., Brinks, D., Adam, Y., Bloxham, W., Kheifets, S., and Cohen, A. E. (2017). Two-photon photoactivated voltage imaging in tissue with an Archaerhodopsin-derived reporter. *bioRxiv*, page 211946.
- [Chong et al., 2017] Chong, E. Z., Barreiros, I., Li, B., Kohl, M. M., and Booth, M. J. (2017). Fast multiplane functional imaging combining acousto-optic switching and remote focusing.
- [Chow et al., 2010] Chow, B. Y., Han, X., Dobry, A. S., Qian, X., Chuong, A. S., Li, M., Henninger, M. A., Belfort, G. M., Lin, Y., Monahan, P. E., and Boyden, E. S. (2010). High-performance genetically targetable optical neural silencing by light-driven proton pumps. *Nature*, 463(7277):98–102.
- [Chowdhury et al., 2010] Chowdhury, F. U., Shah, N., Scarsbrook, A. F., and Bradley, K. M. (2010). [18F]FDG PET/CT imaging of colorectal cancer: A pictorial review. *Postgrad. Med. J.*, 86(1013):174–182.
- [Christensen et al., 2012] Christensen, J. C., Estepp, J. R., Wilson, G. F., and Russell, C. A. (2012). The effects of day-to-day variability of physiological data on operator functional state classification. *Neuroimage*, 59(1):57–63.
- [Clegg, 2010] Clegg, J. (2010). Introduction to Counterpoint.
- [Cohen, 2014] Cohen, A. R. (2014). Extracting meaning from biological imaging data. *Mol. Biol. Cell*, 25(22):3470–3473.
- [Cohen et al., 2009] Cohen, A. R., Bjornsson, C. S., Temple, S., Banker, G., and Roysam, B. (2009). Automatic summarization of changes in biological image sequences using algorithmic information theory. In *IEEE Trans. Pattern Anal. Mach. Intell.*, volume 31, pages 1386–1403. IEEE.
- [Cohen et al., 2010] Cohen, A. R., Gomes, F. L., Roysam, B., and Cayouette, M. (2010). Computational prediction of neural progenitor cell fates. *Nat. Methods*, 7(3):213–218.

- [Cohen and Vitányi, 2015] Cohen, A. R. and Vitányi, P. M. (2015). Normalized compression distance of multisets with applications.
- [Coltuc et al., 2018] Coltuc, D., Datcu, M., and Coltuc, D. (2018). On the Use of Normalized Compression Distances for Image Similarity Detection. *Entropy*, 20:99.
- [Correia and Campilho, 2004a] Correia, M. V. and Campilho, A. (2004a). A Pipelined Real-Time Optical Flow Algorithm. In *International Conference Image Analysis and Recognition*, volume 3212, pages 372–380. Springer.
- [Correia and Campilho, 2004b] Correia, M. V. and Campilho, A. (2004b). A pipelined real-time optical flow algorithm. In *International Conference Image Analysis and Recognition*, pages 372–380. Springer.
- [Cosentino et al., 2016] Cosentino, V., Luis, J., and Cabot, J. (2016). Findings from GitHub. In *Proc. 13th Int. Work. Min. Softw. Repos. - MSR ’16*, pages 137–141. ACM Press.
- [Cribb et al., 2014] Cribb, B., Vishwanath, N., and Upadhyay, V. (2014). Paediatric ovarian lesions—the experience at Starship Children’s Hospital, New Zealand. *N. Z. Med. J.*, 127(1395):41–51.
- [Curnow, 2006] Curnow, W. J. (2006). Bicycle helmets: Lack of efficacy against brain injury. *Accid. Anal. Prev.*, 38(5):833–834.
- [Cusack et al., 2015a] Cusack, R., Vicente-Grabovetsky, A., Mitchell, D. J., Wild, C. J., Auer, T., Linke, A. C., and Peelle, J. E. (2015a). Automatic analysis (aa): efficient neuroimaging workflows and parallel processing using Matlab and XML. *Front. Neuroinform.*, 8.
- [Cusack et al., 2015b] Cusack, R., Vicente-Grabovetsky, A., Mitchell, D. J., Wild, C. J., Auer, T., Linke, A. C., and Peelle, J. E. (2015b). Automatic analysis (aa): efficient neuroimaging workflows and parallel processing using Matlab and XML. *Front. Neuroinform.*, 8.
- [de La Hoz et al., 2016] de La Hoz, E. C., Winter, M. R., Apostolopoulou, M., Temple, S., and Cohen, A. R. (2016). Measuring process dynamics and nuclear migration for clones of neural progenitor cells. In Hua, G. and Jégou, H., editors, *Lect. Notes Comput. Sci. (including Subser. Lect. Notes Artif. Intell. Lect. Notes Bioinformatics)*, volume 9913 LNCS, pages 291–305. Springer International Publishing, Cham.
- [Dehaes et al., 2011] Dehaes, M., Gagnon, L., Lesage, F., Pélégrini-Issac, M., Vignaud, A., Valabregue, R., Grebe, R., Wallois, F., and Benali, H. (2011). Quantitative

- investigation of the effect of the extra-cerebral vasculature in diffuse optical imaging: a simulation study. *Biomed. Opt. Express*, 2(3):680.
- [Deisseroth and Schnitzer, 2013] Deisseroth, K. and Schnitzer, M. J. (2013). Engineering approaches to illuminating brain structure and dynamics. *Neuron*, 80(3):568–577.
- [Diebel, 2006] Diebel, J. (2006). Representing attitude: Euler angles, unit quaternions, and rotation vectors. *Matrix*, 58(15-16):1–35.
- [Dietz and Berthold, 2016] Dietz, C. and Berthold, M. R. (2016). KNIME for open-source bioimage analysis: A tutorial. In *Adv. Anat. Embryol. Cell Biol.*, volume 219 of *Advances in Anatomy, Embryology and Cell Biology*, pages 179–197. Springer, Cham.
- [Dinov et al., 2014] Dinov, I. D., Petrosyan, P., Liu, Z., Eggert, P., Zamanyan, A., Torri, F., Macciardi, F., Hobel, S., Moon, S. W., Sung, Y. H., Jiang, Z., Labus, J., Kurth, F., Ashe-McNalley, C., Mayer, E., Vespa, P. M., Van Horn, J. D., and Toga, A. W. (2014). The perfect neuroimaging-genetics-computation storm: Collision of petabytes of data, millions of hardware devices and thousands of software tools. *Brain Imaging Behav.*, 8(2):311–322.
- [Dombeck et al., 2007] Dombeck, D. A., Khabbaz, A. N., Collman, F., Adelman, T. L., and Tank, D. W. (2007). Imaging Large-Scale Neural Activity with Cellular Resolution in Awake, Mobile Mice. *Neuron*, 56(1):43–57.
- [Doyle et al., 1989] Doyle, H. J., Kraut, R., and Levine, M. (1989). [No Title]. *Genes Dev.*, 3(10):1518–1533.
- [Dragly et al., 2018] Dragly, S.-A., Hobbi Mobarhan, M., Lepperød, M. E., Tennøe, S., Fyhn, M., Hafting, T., and Malthe-Sørenssen, A. (2018). Experimental Directory Structure (Exdir): An Alternative to HDF5 Without Introducing a New File Format. *Front. Neuroinform.*, 12:249979.
- [Dunkels et al., 2006] Dunkels, A., Schmidt, O., Voigt, T., and Ali, M. (2006). Protothreads. *Proc. 4th Int. Conf. Embed. networked Sens. Syst. - SenSys '06*, page 29.
- [El Emam et al., 2002] El Emam, K., Benlarbi, S., Goel, N., Melo, W., Lounis, H., and Rai, S. N. (2002). The optimal class size for object-oriented software. *IEEE Trans. Softw. Eng.*, 28(5):494–509.
- [Electric, 2011] Electric, M. (2011). P2C2 : Programmable Pixel Compressive Camera for High Speed Imaging.
- [Elgabli et al., 2018] Elgabli, A., Aggarwal, V., Hao, S., Qian, F., and Sen, S. (2018). LBP: Robust Rate Adaptation Algorithm for SVC Video Streaming. *IEEE/ACM Trans. Netw.*, 26(4):1633–1645.

- [Elwassif et al., 2006] Elwassif, M. M., Kong, Q., Vazquez, M., and Bikson, M. (2006). Bio-heat transfer model of deep brain stimulation induced temperature changes. *Conf. Proc. ... Annu. Int. Conf. IEEE Eng. Med. Biol. Soc. IEEE Eng. Med. Biol. Soc. Conf.*, 1:3580–3583.
- [Ettrup et al., 2012] Ettrup, K. S., Sørensen, J. C., Rodell, A., Alstrup, A. K., and Bjarkam, C. R. (2012). Hypothalamic deep brain stimulation influences autonomic and limbic circuitry involved in the regulation of aggression and cardiocerebrovascular control in the gttingen minipig. *Stereotact. Funct. Neurosurg.*, 90(5):281–291.
- [Fain et al., 2010] Fain, G. L., Hardie, R., and Laughlin, S. B. (2010). Phototransduction and the evolution of photoreceptors. *Curr. Biol.*, 20(3):R114–R124.
- [Farmer, 1982] Farmer, J. D. (1982). Information Dimension and the Probabilistic Structure of Chaos. *Zeitschrift fur Naturforsch. - Sect. A J. Phys. Sci.*, 37(11):1304–1326.
- [Feng et al., 2007] Feng, X.-j., Greenwald, B., Rabitz, H., Shea-Brown, E., and Kosut, R. (2007). Toward closed-loop optimization of deep brain stimulation for Parkinson’s disease: concepts and lessons from a computational model. *J. Neural Eng.*, 4(2):L14.
- [Ferreira and Rapoport, 2002] Ferreira, A. and Rapoport, M. (2002). The synapsins: Beyond the regulation of neurotransmitter release. *Cell. Mol. Life Sci.*, 59(4):589–595.
- [Flexman et al., 2011] Flexman, M. L., Khalil, M. A., Al Abdi, R., Kim, H. K., Fong, C. J., Desperito, E., Hershman, D. L., Barbour, R. L., and Hielscher, A. H. (2011). Digital optical tomography system for dynamic breast imaging. *J. Biomed. Opt.*, 16(7):076014.
- [Fu et al., 2016] Fu, H., Niu, Z., Zhang, C., Ma, J., and Chen, J. (2016). Visual Cortex Inspired CNN Model for Feature Construction in Text Analysis.
- [Garcia et al., 2014] Garcia, S., Guarino, D., Jaillet, F., Jennings, T., Pröpper, R., Rautenberg, P. L., Rodgers, C. C., Sobolev, A., Wachtler, T., Yger, P., and Davison, A. P. (2014). Neo: an object model for handling electrophysiology data in multiple formats. *Front. Neuroinform.*, 8:10.
- [Grabtchak et al., 2011] Grabtchak, S., Palmer, T. J., and Whelan, W. M. (2011). Detection of localized inclusions of gold nanoparticles in Intralipid-1 *J. Biomed. Opt.*, 16(7):077003.

- [Gradinaru et al., 2009] Gradinaru, V., Mogri, M., Thompson, K. R., Henderson, J. M., and Deisseroth, K. (2009). Optical deconstruction of parkinsonian neural circuitry. *Science (80-.).*, 324(5925):354–359.
- [Gray et al., 2007] Gray, C. M., Goodell, B., and Lear, A. (2007). Multichannel Micromanipulator and Chamber System for Recording Multineuronal Activity in Alert, Non-Human Primates. *J. Neurophysiol.*, 98:527–536.
- [Greenemeier, 2013] Greenemeier, L. (2013). FDA Approves First Retinal Implant. *Nature*.
- [Grienberger and Konnerth, 2012] Grienberger, C. and Konnerth, A. (2012). Imaging Calcium in Neurons. *Neuron*, 73:862–885.
- [Grimm, 2011] Grimm, J. W. (2011). Craving. In Olmstead, M. C., editor, *Anim. Model. Drug Addict.*, number 53 in Neuromethods, pages 311–336. Humana Press.
- [Grossman et al., 2011] Grossman, N., Nikolic, K., Toumazou, C., and Degenaar, P. (2011). Modeling study of the light stimulation of a neuron cell with channelrhodopsin-2 mutants.
- [Grossman et al., 2013] Grossman, N., Simiaki, V., Martinet, C., Toumazou, C., Schultz, S. R., and Nikolic, K. (2013). The spatial pattern of light determines the kinetics and modulates backpropagation of optogenetic action potentials.
- [Grynkiewicz et al., 1985] Grynkiewicz, G., Poenie, M., and Tsien, R. (1985). A New Generation of Ca²⁺-Indicators with Greatly Improved Fluorescence Properties: The Journal of Biological Chemistry. *J. Biol. Chem.*, 260(6):(260)6: 3440–3450.
- [Guizar-Sicairos et al., 2008] Guizar-Sicairos, M., Thurman, S. T., and Fienup, J. R. (2008). Efficient subpixel image registration algorithms. *Opt. Lett.*, 33(2):156.
- [Guo et al., 2014a] Guo, Z. V., Hires, S. A., Li, N., O'Connor, D. H., Komiyama, T., Ophir, E., Huber, D., Bonardi, C., Morandell, K., Gutnisky, D., Peron, S., Xu, N. L., Cox, J., and Svoboda, K. (2014a). Procedures for behavioral experiments in head-fixed mice. *PLoS One*, 9(2):e88678.
- [Guo et al., 2014b] Guo, Z. V., Hires, S. A., Li, N., O'Connor, D. H., Komiyama, T., Ophir, E., Huber, D., Bonardi, C., Morandell, K., Gutnisky, D., Peron, S., Xu, N. L., Cox, J., and Svoboda, K. (2014b). Procedures for behavioral experiments in head-fixed mice. *PLoS One*, 9(2):e88678.
- [Ha et al., 2012] Ha, S., Khraiche, M. L., Silva, G. A., and Cauwenberghs, G. (2012). Direct inductive stimulation for energy-efficient wireless neural interfaces. *Proc. Annu. Int. Conf. IEEE Eng. Med. Biol. Soc. EMBS*, 2012:883–886.

- [Halpern et al., 2011] Halpern, J. H., Sherwood, A. R., Hudson, J. I., Gruber, S., Kozin, D., and Pope, H. G. (2011). Residual neurocognitive features of long-term ecstasy users with minimal exposure to other drugs. *Addiction*, 106:777–786.
- [Hamani et al., 2011] Hamani, C., Mayberg, H., Stone, S., Laxton, A., Haber, S., and Lozano, A. M. (2011). The subcallosal cingulate gyrus in the context of major depression. *Biol. Psychiatry*, 69(4):301–308.
- [Han et al., 2011] Han, X., Chow, B. Y., Zhou, H., Klapoetke, N. C., Chuong, A., Rajimehr, R., Yang, A., Baratta, M. V., Winkle, J., Desimone, R., and Boyden, E. S. (2011). A High-Light Sensitivity Optical Neural Silencer: Development and Application to Optogenetic Control of Non-Human Primate Cortex. *Front. Syst. Neurosci.*, 5:18.
- [Harding et al., 2016] Harding, L. K., Hallinan, G., Milburn, J., Gardner, P., Konidaris, N., Singh, N., Shao, M., Sandhu, J., Kyne, G., and Schlichting, H. E. (2016). CHIMERA: A wide-field, multi-colour, high-speed photometer at the prime focus of the Hale telescope. *Mon. Not. R. Astron. Soc.*, 457(3):3036–3049.
- [Harvey et al., 2012] Harvey, C. D., Coen, P., and Tank, D. W. (2012). Choice-specific sequences in parietal cortex during a virtual-navigation decision task.
- [Harvey et al., 2009] Harvey, C. D., Collman, F., Dombeck, D. A., and Tank, D. W. (2009). Intracellular dynamics of hippocampal place cells during virtual navigation. *Nature*, 461(7266):941–946.
- [Hatsopoulos and Donoghue, 2009] Hatsopoulos, N. G. and Donoghue, J. P. (2009). The Science of Neural Interface Systems. *Annu. Rev. Neurosci.*, 32(1):249–266.
- [He et al., 2015] He, L., Zhang, Y., Ma, G., Tan, P., Li, Z., Zang, S., Wu, X., Jing, J., Fang, S., Zhou, L., Wang, Y., Huang, Y., Hogan, P. G., Han, G., and Zhou, Y. (2015). Near-infrared photoactivatable control of Ca²⁺signaling and optogenetic immunomodulation. *Elife*, 4(DECEMBER2015):e10024.
- [Head et al., 2015] Head, M. L., Holman, L., Lanfear, R., Kahn, A. T., and Jennions, M. D. (2015). The Extent and Consequences of P-Hacking in Science. *PLoS Biol.*, 13:e1002106.
- [Hense et al., 2015] Hense, A., Prunsche, B., Gao, P., Ishitsuka, Y., Nienhaus, K., and Nienhaus, G. U. (2015). Monomeric Garnet, a far-red fluorescent protein for live-cell STED imaging. *Sci. Rep.*, 5:18006.
- [Herman et al., 2017] Herman, M. C., Cardoso, M. M. B., Lima, B., Sirotin, Y. B., and Das, A. (2017). Simultaneously estimating the task-related and stimulus-evoked components of hemodynamic imaging measurements. *Neurophotonics*, 4(3):031223.

- [Hernández et al., 2018a] Hernández, S. C., Jiménez, L. D., and García, J. A. B. (2018a). Potential of energy production from slaughterhouse wastewater. *Interciencia*, 43(8):558–565.
- [Hernández et al., 2018b] Hernández, S. C., Jiménez, L. D., and García, J. A. B. (2018b). Potential of energy production from slaughterhouse wastewater. *Interciencia*, 43(8):558–565.
- [Hilbert and López, 2012] Hilbert, M. and López, P. (2012). How to measure the world’s technological capacity to communicate, store, and compute information, part I: Results and scope. *Int. J. Commun.*, 6:956–979.
- [Hillman, 2007] Hillman, E. M. C. (2007). Optical brain imaging in vivo: techniques and applications from animal to man. *J. Biomed. Opt.*, 12(5):051402.
- [Hirsch et al., 2009] Hirsch, M., Lanman, D., Holtzman, H., and Raskar, R. (2009). BiDi screen.
- [Hodneland et al., 2013a] Hodneland, E., Kögel, T., Frei, D. M., Gerdes, H. H., and Lundervold, A. (2013a). CellSegm - a MATLAB toolbox for high-throughput 3D cell segmentation. *Source Code Biol. Med.*, 8:16.
- [Hodneland et al., 2013b] Hodneland, E., Kögel, T., Frei, D. M., Gerdes, H. H., and Lundervold, A. (2013b). CellSegm - a MATLAB toolbox for high-throughput 3D cell segmentation. *Source Code Biol. Med.*, 8:16.
- [Hoffmann and Reitz, 2018] Hoffmann, O. and Reitz, F. (2018). Hdblp: Historical Data of the Dblp Collection.
- [Holekamp et al., 2008a] Holekamp, T. F., Turaga, D., and Holy, T. E. (2008a). Fast Three-Dimensional Fluorescence Imaging of Activity in Neural Populations by Objective-Coupled Planar Illumination Microscopy. *Neuron*, 57(5):661–672.
- [Holekamp et al., 2008b] Holekamp, T. F., Turaga, D., and Holy, T. E. (2008b). Fast Three-Dimensional Fluorescence Imaging of Activity in Neural Populations by Objective-Coupled Planar Illumination Microscopy. *Neuron*, 57:661–672.
- [Honari et al., 2017] Honari, S., Molchanov, P., Tyree, S., Vincent, P., Pal, C., and Kautz, J. (2017). Improving Landmark Localization with Semi-Supervised Learning. *arXiv1709.01591 [cs]*.
- [Hong et al., 2004] Hong, V., Palus, H., and Paulus, D. (2004). Edge preserving filters on color images. *Comput. Sci. - ICCS 2004*, pages 34–40.
- [Hu et al., 2016] Hu, Y., Zhang, J., Bai, X., Yu, S., and Yang, Z. (2016). Influence analysis of Github repositories. *Springerplus*, 5(1):1268.

- [Huanglin Zeng et al., 1992] Huanglin Zeng, Juebang Yu, and Guiging He (1992). Stability analysis on continuous neural networks with slowly synapse-varying structure. In *[Proceedings] 1992 IEEE Int. Symp. Circuits Syst.*, volume 1, pages 443–446.
- [Iancu et al., 2005] Iancu, R., Mohapel, P., Brundin, P., and Paul, G. (2005). Behavioral characterization of a unilateral 6-OHDA-lesion model of Parkinson’s disease in mice. *Behav. Brain Res.*, 162(1):1–10.
- [Ince et al., 2010a] Ince, R. A., Mazzoni, A., Petersen, R. S., and Panzeri, S. (2010a). Open source tools for the information theoretic analysis of neural data. *Front. Neurosci.*, 4(MAY):62–70.
- [Ince et al., 2010b] Ince, R. A., Mazzoni, A., Petersen, R. S., and Panzeri, S. (2010b). Open source tools for the information theoretic analysis of neural data. *Front. Neurosci.*, 4(MAY):62–70.
- [Ince et al., 2015] Ince, R. A., Van Rijsbergen, N. J., Thut, G., Rousselet, G. A., Gross, J., Panzeri, S., and Schyns, P. G. (2015). Tracing the Flow of Perceptual Features in an Algorithmic Brain Network. *Sci. Rep.*, 5:17681.
- [Ince et al., 2014] Ince, R. A. A., Schultz, S. R., and Panzeri, S. (2014). Estimating Information-Theoretic Quantities. *Encycl. Comput. Neurosci.*, pages 1–13.
- [Intan, 2013] Intan (2013). Intan Technologies: Integrated Amplifiers for Electrophysiology and Biosensing.
- [Ishikawa et al., 2010] Ishikawa, D., Takahashi, N., Sasaki, T., Usami, A., Matsuki, N., and Ikegaya, Y. (2010). Fluorescent pipettes for optically targeted patch-clamp recordings. *Neural Networks*, 23(6):669–672.
- [Jackson and Muthuswamy, 2008] Jackson, N. and Muthuswamy, J. (2008). Artificial dural sealant that allows multiple penetrations of implantable brain probes. *J. Neurosci. Methods*, 171(1):147–152.
- [Jacoby et al., 2014] Jacoby, J., Kreitzer, M. A., Alford, S., and Malchow, R. P. (2014). Fluorescent imaging reports an extracellular alkalinization induced by glutamatergic activation of isolated retinal horizontal cells. *J. Neurophysiol.*, 111(5):1056–1064.
- [Jacomy et al., 2014] Jacomy, M., Venturini, T., Heymann, S., and Bastian, M. (2014). ForceAtlas2, a continuous graph layout algorithm for handy network visualization designed for the Gephi software. *PLoS One*, 9(6):e98679.
- [Jain and Chlamtac, 1985] Jain, R. and Chlamtac, I. (1985). The P2 algorithm for dynamic calculation of quantiles and histograms without storing observations. *Commun. ACM*, 28(10):1076–1085.

- [James et al., 2017] James, R., Chebee7i, Harper, M., Ince, R., and Delicious., M. G. (2017). Dit/Dit V1.0.0.Dev14. Technical report, Zenodo.
- [Jamison et al., 2015] Jamison, K. W., Roy, A. V., He, S., Engel, S. A., and He, B. (2015). SSVEP signatures of binocular rivalry during simultaneous EEG and fMRI. *J. Neurosci. Methods*, 243:53–62.
- [Jarvis et al., 2006] Jarvis, R. M., Broadhurst, D., Johnson, H., O’Boyle, N. M., and Goodacre, R. (2006). PYCHEM: A multivariate analysis package for python. *Bioinformatics*, 22(20):2565–2566.
- [Ji et al., 2016] Ji, N., Freeman, J., and Smith, S. L. (2016). Technologies for imaging neural activity in large volumes. *Nat. Neurosci.*, 19(9):1154–1164.
- [Jia et al., 2011] Jia, Z., Valiunas, V., Lu, Z., Bien, H., Liu, H., Wang, H.-Z., Rosati, B., Brink, P. R., Cohen, I. S., and Entcheva, E. (2011). Stimulating Cardiac Muscle by Light: Cardiac Optogenetics by Cell Delivery. *Circ. Arrhythmia Electrophysiol.*
- [Jones et al., 2010] Jones, A. P., Happé, F. G., Gilbert, F., Burnett, S., and Viding, E. (2010). Feeling, caring, knowing: different types of empathy deficit in boys with psychopathic tendencies and autism spectrum disorder. *J. Child Psychol. Psychiatry*, 51(11):1188–1197.
- [Jurkowitsch and Knobler, 2008] Jurkowitsch, T. and Knobler, R. (2008). Light Treatment in Medicine. In Björn, L. O., editor, *Photobiology*, pages 577–590. Springer New York, New York, NY.
- [Kang and Lowery, 2013] Kang, G. and Lowery, M. M. (2013). Interaction of oscillations, and their suppression via deep brain stimulation, in a model of the cortico-basal ganglia network. *IEEE Trans. Neural Syst. Rehabil. Eng.*, 21(2):244–253.
- [Khaleghi et al., 2015] Khaleghi, A., Sheikhani, A., Mohammadi, M. R., and Nasrabadi, A. M. (2015). Evaluation of cerebral cortex function in clients with bipolar mood disorder I (BMD I) compared with BMD II using QEEG analysis.
- [Kienzler, 2017] Kienzler, R. (2017). Developing cognitive IoT solutions for anomaly detection by using deep learning, Part 1: Introducing deep learning and long-short term memory networks Detecting anomalies in IoT time-series data by using deep learning.
- [Kikuchi et al., 2017] Kikuchi, T., Morizane, A., Doi, D., Magotani, H., Onoe, H., Hayashi, T., Mizuma, H., Takara, S., Takahashi, R., Inoue, H., Morita, S., Yamamoto, M., Okita, K., Nakagawa, M., Parmar, M., and Takahashi, J. (2017). Human iPS cell-derived dopaminergic neurons function in a primate Parkinson’s disease model. *Nature*, 548(7669):592–596.

- [Kim et al., 2015] Kim, K. M., Son, K., and Palmore, G. T. R. (2015). Neuron image analyzer: Automated and accurate extraction of neuronal data from low quality images. *Sci. Rep.*, 5:srep17062.
- [Klein et al., 2013] Klein, T. A., Ullsperger, M., and Danielmeier, C. (2013). Error awareness and the insula: links to neurological and psychiatric diseases. *Front. Hum. Neurosci.*, 7:14.
- [Knöpfel, 2012] Knöpfel, T. (2012). Genetically encoded optical indicators for the analysis of neuronal circuits. *Nat. Rev. Neurosci.*, 13:687–700.
- [Kobayashi et al., 2012] Kobayashi, T., Motoyama, M., Masuda, H., Ohta, Y., Haruta, M., Noda, T., Sasagawa, K., Tokuda, T., Tamura, H., Ishikawa, Y., Shiosaka, S., and Ohta, J. (2012). Novel implantable imaging system for enabling simultaneous multiplanar and multipoint analysis for fluorescence potentiometry in the visual cortex. *Biosens. Bioelectron.*, 38(1):321–330.
- [Kocz et al., 2014] Kocz, J., Greenhill, L. J., Barsdell, B. R., Price, D., Bernardi, G., Bourke, S., Clark, M. A., Craig, J., Dexter, M., Dowell, J., Eftekhari, T., Ellingson, S., Hallinan, G., Hartman, J., Jameson, A., MacMahon, D., Taylor, G., Schinzel, F., and Werthimer, D. (2014). Digital Signal Processing using Stream High Performance Computing: A 512-input Broadband Correlator for Radio Astronomy. *J. Astron. Instrum.*, 04(01n02):1550003.
- [Kondabolu et al., 2016] Kondabolu, K., Roberts, E. A., Bucklin, M., McCarthy, M. M., Kopell, N., and Han, X. (2016). Striatal cholinergic interneurons generate beta and gamma oscillations in the corticostriatal circuit and produce motor deficits. *Proceedings of the National Academy of Sciences*, 113(22):E3159–E3168.
- [Krack et al., 2010] Krack, P., Hariz, M. I., Baunez, C., Guridi, J., and Obeso, J. A. (2010). Deep brain stimulation: from neurology to psychiatry? *Trends Neurosci.*, 33(10):474–484.
- [Krawinkel et al., 2015] Krawinkel, L. A., Engel, A. K., and Hummel, F. C. (2015). Modulating pathological oscillations by rhythmic non-invasive brain stimulation—a therapeutic concept? *Front. Syst. Neurosci.*, 9:33.
- [Krüger and Westermann, 2003] Krüger, J. and Westermann, R. (2003). Linear algebra operators for GPU implementation of numerical algorithms. In *ACM Trans. Graph.*, number 3 in SIGGRAPH '05, page 908, New York, NY, USA. ACM.
- [Kuhlmann, 2000] Kuhlmann, U. (2000). [No Title]. *J. Mol. Biol.*, 301(5):1163–1178.
- [Lakhssassi et al., 2010] Lakhssassi, A., Kengne, E., and Semmaoui, H. (2010). Modified pennes' equation modelling bio-heat transfer in living tissues: analytical and numerical analysis. *Nat. Sci.*, 02(12):1375–1385.

- [Lang, 2017] Lang, K. J. (2017). Back to the Future: an Even More Nearly Optimal Cardinality Estimation Algorithm.
- [Larson and larsonp neurosurg ucsf edu Larson, 2008] Larson, P. S. E. M. A. and larsonp neurosurg ucsf edu Larson, P. S. (2008). Deep brain stimulation for psychiatric disorders. [References]. *Neurotherapeutics*, .5:289–307.
- [Leach, 2010] Leach, J. (2010). Bridging the divide between neuroprosthetic design, tissue engineering and neurobiology. *Front. Neuroeng.*, 2:18.
- [Li and Andrews, 2007] Li, J. and Andrews, R. J. (2007). Trimodal nanoelectrode array for precise deep brain stimulation: Prospects of a new technology based on carbon nanofiber arrays. In *Acta Neurochir. Suppl.*, number 97 PART 2 in *Acta Neurochirurgica Supplements*, pages 537–545. Springer Vienna.
- [Li et al., 2018a] Li, L., Mi, Y., Zhang, W., Wang, D.-H., and Wu, S. (2018a). Dynamic Information Encoding With Dynamic Synapses in Neural Adaptation. *Front. Comput. Neurosci.*, 12:16.
- [Li et al., 2018b] Li, R., Wang, M., Yao, J., Liang, S., Liao, X., Yang, M., Zhang, J., Yan, J., Jia, H., Chen, X., and Li, X. (2018b). Two-Photon Functional Imaging of the Auditory Cortex in Behaving Mice: From Neural Networks to Single Spines. *Front. Neural Circuits*, 12.
- [Liker et al., 2008] Liker, M. A., Rao, V. Y., Hua, S. E., Won, D. S., and Won, D. S. (2008). Deep Brain Stimulation: An Evolving Technology. *Proc. IEEE*, 96:1129–1141.
- [Lillis et al., 2008] Lillis, K. P., Eng, A., White, J. A., and Mertz, J. (2008). Two-photon imaging of spatially extended neuronal network dynamics with high temporal resolution. *J. Neurosci. Methods*, 172(2):178–184.
- [Lin et al., 2015] Lin, Q., Ooi, B. C., Wang, Z., and Yu, C. (2015). Scalable Distributed Stream Join Processing. *Proc. 2015 ACM SIGMOD Int. Conf. Manag. Data - SIGMOD '15*, pages 811–825.
- [Liston et al., 2008] Liston, A., Enders, A., and Siggs, O. M. (2008). Unravelling the association of partial T-cell immunodeficiency and immune dysregulation. *Nat. Rev. Immunol.*, 8(7):545–558.
- [Lizier, 2014] Lizier, J. T. (2014). JIDT: An information-theoretic toolkit for studying the dynamics of complex systems. *Front. Robot. AI*, 1.
- [Looks et al., 2017] Looks, M., Herreshoff, M., Hutchins, D., and Norvig, P. (2017). Deep Learning with Dynamic Computation Graphs.

- [Louis et al., 2010] Louis, S., Borgelt, C., and Grün, S. (2010). Complexity distribution as a measure for assembly size and temporal precision. *Neural Networks*, 23(6):705–712.
- [Loweth and Vezina, 2011] Loweth, J. A. and Vezina, P. (2011). Sensitization. In Olmstead, M. C., editor, *Anim. Model. Drug Addict.*, number 53 in Neuromethods, pages 191–205. Humana Press.
- [Lozano et al., 2012] Lozano, A. M., Giacobbe, P., Hamani, C., Rizvi, S. J., Kennedy, S. H., Kolivakis, T. T., Debonnel, G., Sadikot, A. F., Lam, R. W., and Howard, A. K. (2012). A multicenter pilot study of subcallosal cingulate area deep brain stimulation for treatment-resistant depression. *J. Neurosurg.*, 116(2):315–322.
- [Lozano et al., 2008] Lozano, A. M., Mayberg, H. S., Giacobbe, P., Hamani, C., Craddock, R. C., and Kennedy, S. H. (2008). Subcallosal cingulate gyrus deep brain stimulation for treatment-resistant depression. *Biol. Psychiatry*, 64(6):461–467.
- [Loze and Wright, 2001] Loze, M. K. and Wright, C. D. (2001). Temperature distributions in laser-heated biological tissue with application to birthmark removal. *J. Biomed. Opt.*, 6(1):74.
- [Ludwig, 1950] Ludwig, G. D. (1950). The Velocity of Sound through Tissues and the Acoustic Impedance of Tissues. *J. Acoust. Soc. Am.*, 22(6):862–866.
- [Luebke et al., 2004] Luebke, D., Harris, M., Krüger, J., Purcell, T., Govindaraju, N., Buck, I., Woolley, C., and Lefohn, A. (2004). Gpgpu. In *Proc. Conf. SIGGRAPH 2004 course notes - GRAPH '04*, SIGGRAPH '04, pages 33–es, New York, NY, USA. ACM.
- [Luigjes et al., 2012] Luigjes, J., van den Brink, W., Feenstra, M., van den Munckhof, P., Schuurman, P. R., Schippers, R., Mazaheri, A., Vries, T. J. D., and Denys, D. (2012). Deep brain stimulation in addiction: a review of potential brain targets. *Mol. Psychiatry*, 17(6):572–583.
- [Ma et al., 2013a] Ma, C., Cao, X., Tong, X., Dai, Q., and Lin, S. (2013a). Acquisition of High Spatial and Spectral Resolution Video with a Hybrid Camera System. *Int. J. Comput. Vis.*, 110(2):141–155.
- [Ma et al., 2013b] Ma, C., Cao, X., Tong, X., Dai, Q., and Lin, S. (2013b). Acquisition of High Spatial and Spectral Resolution Video with a Hybrid Camera System. *Int. J. Comput. Vis.*, 110(2):141–155.
- [Ma et al., 2010] Ma, Y., Galinski, E. A., Grant, W. D., Oren, A., and Ventosa, A. (2010). Halophiles 2010: Life in saline environments. *Appl. Environ. Microbiol.*, 76(21):6971–6981.

- [Machado and Balbinot, 2014] Machado, J. and Balbinot, A. (2014). Executed movement using EEG signals through a naive bayes classifier. *Micromachines*, 5(4):1082–1105.
- [Madisen et al., 2015] Madisen, L., Garner, A. R., Shimaoka, D., Chuong, A. S., Klapoetke, N. C., Li, L., van der Bourg, A., Niino, Y., Egolf, L., Monetti, C., Gu, H., Mills, M., Cheng, A., Tasic, B., Nguyen, T. N., Sunkin, S. M., Benucci, A., Nagy, A., Miyawaki, A., Helmchen, F., Empson, R. M., Knöpfel, T., Boyden, E. S., Reid, R. C., Carandini, M., and Zeng, H. (2015). Transgenic mice for intersectional targeting of neural sensors and effectors with high specificity and performance. *Neuron*, 85:942–958.
- [Maia and Silva, 2017] Maia, A. d. O. and Silva, D. A. (2017). Proposal to Use of the WebSocket Protocol for Web Device Control. *Proc. 23rd Brazillian Symp. Multimed. Web - WebMedia '17*, pages 253–260.
- [Malone et al., 2009] Malone, D. A. J., Dougherty, D. D., Rezai, A. R., Carpenter, L. L., Friehs, G. M., Eskandar, E. N., Rauch, S. L., Rasmussen, S. A., Machado, A. G., Kubu, C. S., Tyrka, A. R., Price, L. H., Stypulkowski, P. H., Giftakis, J. E., Rise, M. T., Malloy, P. F., Salloway, S. P., and Greenberg, B. D. (2009). Deep Brain Stimulation of the Ventral Capsule/Ventral Striatum for Treatment-Resistant Depression. *Bps*, 65(4):267–275.
- [Maltsev et al., 2017] Maltsev, A. V., Parsons, S. P., Kim, M. S., Tsutsui, K., Stern, M. D., Lakatta, E. G., Maltsev, V. A., and Monfredi, O. (2017). Computer algorithms for automated detection and analysis of local Ca²⁺releases in spontaneously beating cardiac pacemaker cells. *PLoS One*, 12(7):e0179419.
- [Mantione et al., 2010] Mantione, M., Van De Brink, W., Schuurman, P. R., and Denys, D. (2010). Smoking cessation and weight loss after chronic deep brain stimulation of the nucleus accumbens: Therapeutic and research implications: Case report. *Neurosurgery*, 66(1):E218; discussion E218.
- [Mattis et al., 2012] Mattis, J., Tye, K. M., Ferenczi, E. A., Ramakrishnan, C., O’Shea, D. J., Prakash, R., Gunaydin, L. A., Hyun, M., Fenno, L. E., Gradinaru, V., Yizhar, O., and Deisseroth, K. (2012). Principles for applying optogenetic tools derived from direct comparative analysis of microbial opsins. *Nat. Methods*, 9(2):159–172.
- [Mazhar et al., 2017] Mazhar, O., Jamaluddin, A. Z., Jiang, C., Fofi, D., Seulin, R., and Morel, O. (2017). Design and Calibration of a Specialized Polydioptric Camera Rig. *Front. ICT*, 4.
- [McLelland et al., 2015] McLelland, A. E., Winkler, C. E., and Martin-Iverson, M. T. (2015). A simple and effective method for building inexpensive infrared

- equipment used to monitor animal locomotion. *Journal of Neuroscience Methods*, 243:1–7.
- [McNeely et al., 2008] McNeely, H. E., Mayberg, H. S., Lozano, A. M., and Kennedy, S. H. (2008). Neuropsychological impact of Cg25 deep brain stimulation for treatment-resistant depression: preliminary results over 12 months. *J. Nerv. Ment. Dis.*, 196(5):405–410.
- [McQuin et al., 2018] McQuin, C., Goodman, A., Chernyshev, V., Kamentsky, L., Cimini, B. A., Karhohs, K. W., Doan, M., Ding, L., Rafelski, S. M., Thirstrup, D., Wiegraebe, W., Singh, S., Becker, T., Caicedo, J. C., and Carpenter, A. E. (2018). CellProfiler 3.0: Next-generation image processing for biology. *PLoS Biol.*, 16(7):1–17.
- [Mendhurwar et al., 2018] Mendhurwar, K., Gu, Q., Mudur, S., and Popa, T. (2018). The Discriminative Power of Shape an Empirical Study in Time Series Matching. *IEEE Trans. Vis. Comput. Graph.*, 24(5):1799–1813.
- [Meyer and Tischer, 2001] Meyer, B. and Tischer, P. E. (2001). Glicbawls - Grey Level Image Compression by Adaptive Weighted Least Squares. *Data Compression Conf.*, page 503.
- [Michelozzi et al., 2000] Michelozzi, P., Forastiere, F., Perucci, C. A., Fusco, D., Barca, A., and Spadea, T. (2000). Studi sugli effetti acuti dell'inquinamento atmosferico a Roma. *Ann. Ist. Super. Sanita*, 36(3):297–304.
- [Miller et al., 2012] Miller, J. S., Stevens, K. R., Yang, M. T., Baker, B. M., Nguyen, D.-H. T., Cohen, D. M., Toro, E., Chen, A. A., Galie, P. A., Yu, X., Chaturvedi, R., Bhatia, S. N., and Chen, C. S. (2012). Rapid casting of patterned vascular networks for perfusable engineered three-dimensional tissues. *Nat. Mater.*, 11(9):768–774.
- [Milovanov and Vereshchagin, 2017] Milovanov, A. and Vereshchagin, N. (2017). Stochasticity in algorithmic statistics for polynomial time. *Leibniz Int. Proc. Informatics, LIPIcs*, 79(43):1–21.
- [Min et al., 2012] Min, G., Kim, J. W., Choi, W. J., and Lee, B. H. (2012). Numerical correction of distorted images in full-field optical coherence tomography. *Meas. Sci. Technol.*, 23(3).
- [Miró Julià, 2011] Miró Julià, J. (2011). An engineering approach to teaching writing. In *Proc. 42nd ACM Tech. Symp. Comput. Sci. Educ.*, pages 535–540, New York, New York, USA. ACM Press.

- [Mohammed et al., 2016] Mohammed, A. I., Gritton, H. J., Tseng, H. A., Bucklin, M. E., Yao, Z., and Han, X. (2016). An integrative approach for analyzing hundreds of neurons in task performing mice using wide-field calcium imaging. *Sci. Rep.*, 6.
- [Mohd et al., 2017a] Mohd, S., Brahim, J., Latiffi, A. A., Fathi, M. S., and Harun, A. N. (2017a). Developing building information modelling (BIM) implementation model for project design team. *Malaysian Constr. Res. J.*, 1(1):71–83.
- [Mohd et al., 2017b] Mohd, S., Brahim, J., Latiffi, A. A., Fathi, M. S., and Harun, A. N. (2017b). Developing building information modelling (BIM) implementation model for project design team. *Malaysian Constr. Res. J.*, 1(1):71–83.
- [Monteforte and Wolf, 2010] Monteforte, M. and Wolf, F. (2010). Dynamical entropy production in spiking neuron networks in the balanced state. *Phys. Rev. Lett.*, 105(26):268104.
- [Moore et al., 2010] Moore, T. L., Killiany, R. J., Pessina, M. A., Moss, M. B., and Rosene, D. L. (2010). Assessment of motor function of the hand in aged rhesus monkeys. *Somatosens. Mot. Res.*, 27(3):121–130.
- [Moran et al., 2016] Moran, J., Alexander, M. L., and Laskin, A. (2016). Soil Carbon: Compositional and Isotopic Analysis. *Encycl. Soil Sci. Third Ed.*, pages 2073–2077.
- [Morant II, 2012] Morant II, W. (2012). Blackboard Academic Suite.
- [Morris et al., 2004] Morris, K., O'Brien, T. J., Cook, M. J., Murphy, M., and Bowden, S. C. (2004). A Computer-Generated Stereotactic "Virtual Subdural Grid" to Guide Resective Epilepsy Surgery.
- [Mourot et al., 2013] Mourot, A., Tochitsky, I., and Kramer, R. H. (2013). Light at the end of the channel: optical manipulation of intrinsic neuronal excitability with chemical photoswitches. *Front. Mol. Neurosci.*, 6:5.
- [Mukamel et al., 2009] Mukamel, E. A., Nimmerjahn, A., and Schnitzer, M. J. (2009). Automated Analysis of Cellular Signals from Large-Scale Calcium Imaging Data. *Neuron*, 63(6):747–760.
- [Mullapudi et al., 2016] Mullapudi, R. T., Adams, A., Sharlet, D., Ragan-Kelley, J., and Fatahalian, K. (2016). Automatically scheduling halide image processing pipelines. *ACM Trans. Graph.*, 35(4):1–11.
- [Munegowda and Raju Professor, 2011] Munegowda, K. and Raju Professor, G. T. (2011). The Extended FAT file system.

- [Murari et al., 2010] Murari, K., Etienne-Cummings, R., Cauwenberghs, G., and Thakor, N. (2010). An integrated imaging microscope for untethered cortical imaging in freely-moving animals. In *2010 Annu. Int. Conf. IEEE Eng. Med. Biol. Soc. EMBC'10*, pages 5795–5798. IEEE.
- [Narang et al., 2017] Narang, S., Diamos, G., Sengupta, S., and Elsen, E. (2017). Exploring Sparsity in. *Iclr*, pages 1–10.
- [Ng et al., 2006] Ng, D. C., Tamura, H., Tokuda, T., Yamamoto, A., Matsuo, M., Nunoshita, M., Ishikawa, Y., Shiosaka, S., and Ohta, J. (2006). Real time in vivo imaging and measurement of serine protease activity in the mouse hippocampus using a dedicated complementary metal-oxide semiconductor imaging device. *J. Neurosci. Methods*, 156(1-2):23–30.
- [Nguyen et al., 2016] Nguyen, V., Rizzo, J., and Sanii, B. (2016). An assemblable, multi-angle fluorescence and ellipsometric microscope. *PLoS One*, 11.
- [Nieh et al., 2013] Nieh, E. H., Kim, S. Y., Namburi, P., and Tye, K. M. (2013). Optogenetic dissection of neural circuits underlying emotional valence and motivated behaviors. *Brain Res.*, 1511:73–92.
- [Niitani et al., 2017] Niitani, Y., Ogawa, T., Saito, S., and Saito, M. (2017). ChainerCV: a Library for Deep Learning in Computer Vision. *arXiv1708.08169 [cs]*.
- [Niklaus et al., 2017] Niklaus, S., Mai, L., and Liu, F. (2017). Video Frame Interpolation via Adaptive Separable Convolution. *arXiv1708.01692 [cs]*.
- [Nowinski et al., 2000] Nowinski, W. L., Yang, Q. L., and Yeo, T. T. (2000). Computer-aided stereotactic functional neurosurgery enhanced by the use of the multiple brain atlas database. *IEEE Trans. Med. Imaging*, 19(1):62–69.
- [Ohayon et al., 2017] Ohayon, S., Caravaca-Aguirre, A. M., Piestun, R., and DiCarlo, J. J. (2017). Deep brain fluorescence imaging with minimally invasive ultra-thin optical fibers. *arXiv Prepr. arXiv1703.07633*, page 116350.
- [O’Leary et al., 2018] O’Leary, J. D., O’Leary, O. F., Cryan, J. F., and Nolan, Y. M. (2018). A low-cost touchscreen operant chamber using a Raspberry PiTM.
- [Oroudi, 2011] Oroudi, I. M. (2011). Evaporation estimates from the Dead Sea and their implications on its water balance. *Theor. Appl. Climatol.*, 106(3-4):523–530.
- [Packer et al., 2013] Packer, A. M., Roska, B., and Häuser, M. (2013). Targeting neurons and photons for optogenetics. *Nat. Neurosci.*, 16:805–815.
- [Palmer, 2015] Palmer, T. (2015). Modelling: Build imprecise supercomputers. *Nature*, 526(7571):32–33.

- [Papo, 2016] Papo, D. (2016). Commentary: The entropic brain: a theory of conscious states informed by neuroimaging research with psychedelic drugs. *Front. Hum. Neurosci.*, 10:20.
- [Park et al., 2015] Park, C., Woehl, T. J., Evans, J. E., and Browning, N. D. (2015). Minimum cost multi-way data association for optimizing multitarget tracking of interacting objects. *IEEE Trans. Pattern Anal. Mach. Intell.*, 37(3):611–624.
- [Patel et al., 2017a] Patel, Y. A., George, A., Dorval, A. D., White, J. A., Christini, D. J., and Butera, R. J. (2017a). Hard real-time closed-loop electrophysiology with the Real-Time eXperiment Interface (RTXI). *PLoS Comput. Biol.*, 13(5):e1005430.
- [Patel et al., 2017b] Patel, Y. A., George, A., Dorval, A. D., White, J. A., Christini, D. J., and Butera, R. J. (2017b). Hard real-time closed-loop electrophysiology with the Real-Time eXperiment Interface (RTXI). *PLoS Comput. Biol.*, 13(5):e1005430.
- [Pébay, 2008] Pébay, P. (2008). Formulas for Robust, One-Pass Parallel Computation of Covariances and Arbitrary-Order Statistical Moments. *Sandia Rep. SAND2008-6212*, Sandia Natl. Lab., 94(September).
- [Pestilli, 2015] Pestilli, F. (2015). Test-retest measurements and digital validation for in vivo neuroscience. *Sci. Data*, 2:140057.
- [Philibin et al., 2011] Philibin, S. D., Hernandez, A., Self, D. W., and Bibb, J. A. (2011). Striatal Signal Transduction and Drug Addiction. *Front. Neuroanat.*, 5:60.
- [Polikov et al., 2005] Polikov, V. S., Tresco, P. A., and Reichert, W. M. (2005). Response of brain tissue to chronically implanted neural electrodes. *J. Neurosci. Methods*, 148(1):1–18.
- [Powers and Tony Brown, 1986] Powers, S. K. and Tony Brown, J. (1986). Light dosimetry in brain tissue: An in vivo model applicable to photodynamic therapy. *Lasers Surg. Med.*, 6(3):318–322.
- [Press and Uide, 2008] Press, U. and Uide, P. R. S. G. (2008). Usbx p ’ g. *Library (Lond)*., pages 1–36.
- [Prinz and Priller, 2017] Prinz, M. and Priller, J. (2017). The role of peripheral immune cells in the CNS in steady state and disease. *Nat. Neurosci.*, 20(2):136–144.
- [Programming, 2010] Programming, C. V. (2010). External Interfaces. *MATLAB Prim. Eighth Ed.*, pages 211–211.
- [Quérard et al., 2017] Quérard, J., Zhang, R., Kelemen, Z., Plamont, M. A., Xie, X., Chouket, R., Roemgens, I., Korepina, Y., Albright, S., Ipendey, E., Volovitch, M., Sladitschek, H. L., Neveu, P., Gissot, L., Gautier, A., Faure, J. D., Croquette, V.,

- Le Saux, T., and Jullien, L. (2017). Resonant out-of-phase fluorescence microscopy and remote imaging overcome spectral limitations.
- [Raafat et al., 2017] Raafat, H. M., Hossain, M. S., Essa, E., Elmougy, S., Tolba, A. S., Muhammad, G., and Ghoneim, A. (2017). Fog Intelligence for Real-Time IoT Sensor Data Analytics. *IEEE Access*, 5:24062–24069.
- [Rainey et al., 2014] Rainey, E., Villarreal, J., Dedeoglu, G., Pulli, K., Lepley, T., and Brill, F. (2014). Addressing system-level optimization with openVX graphs. In *IEEE Comput. Soc. Conf. Comput. Vis. Pattern Recognit. Work.*, pages 658–663.
- [Ramdhani et al., 2018] Ramdhani, R. A., Khojandi, A., Shylo, O., and Kopell, B. (2018). Optimizing Clinical Assessments in Parkinson’s Disease Through The Use of Wearable Sensors and Data Driven Modeling. *Front. Comput. Neurosci.*, 12:72.
- [Rao et al., 2013] Rao, V. I., Bhat, K. G., Pai, V., Rao, S. P., and Shantaram, M. (2013). Effect of mupirocin treatment on nasal carriage of methicillin resistant *Staphylococcus aureus* in hospital healthcare workers. *Biomed.*, 33(1):110–112.
- [Rapp et al., 2002a] Rapp, G. E., Barbosa Júnior, A. d. A., Mendes, A. J. D., Motta, A. C. F., Bião, M. A. d. A., and Garcia, R. V. (2002a). Technical assessment of WHO-621 periodontal probe made in Brazil. *Braz. Dent. J.*, 13(1):61–65.
- [Rapp et al., 2002b] Rapp, G. E., Barbosa Júnior, A. d. A., Mendes, A. J. D., Motta, A. C. F., Bião, M. A. d. A., and Garcia, R. V. (2002b). Technical assessment of WHO-621 periodontal probe made in Brazil. *Braz. Dent. J.*, 13(1):61–65.
- [Ratzlaff and Grinvald, 1991] Ratzlaff, E. H. and Grinvald, A. (1991). A tandem-lens epifluorescence macroscope: Hundred-fold brightness advantage for wide-field imaging. *J. Neurosci. Methods*, 36(2-3):127–137.
- [Reed and Kaas, 2010] Reed, J. L. and Kaas, J. H. (2010). Statistical analysis of large-scale neuronal recording data. *Neural Networks*, 23:673–684.
- [Reichert et al., 2007] Reichert, T., Latour, M. S., Lambiase, J. J., and Adkins, M. (2007). A test of media literacy effects and sexual objectification in advertising. *J. Curr. Issues Res. Advert.*, 29(1):81–92.
- [Richards and Frankland, 2017] Richards, B. A. and Frankland, P. W. (2017). The Persistence and Transience of Memory. *Neuron*, 94(6):1071–1084.
- [Richman and Moorman, 2000] Richman, J. S. and Moorman, J. R. (2000). Physiological time-series analysis using approximate entropy and sample entropy. *Am. J. Physiol. Circ. Physiol.*, 278(6):H2039–H2049.

- [Robinson et al., 2013] Robinson, J. T., Jorgolli, M., and Park, H. (2013). Nanowire electrodes for high-density stimulation and measurement of neural circuits. *Front. Neural Circuits*, 7:38.
- [Romano et al., 2019] Romano, M., Bucklin, M., Gritton, H., Mehrotra, D., Kessel, R., and Han, X. (2019). A teensy microcontroller-based interface for optical imaging camera control during behavioral experiments. *Journal of Neuroscience Methods*, 320:107–115.
- [Rubenzer, 2010] Rubenzer, S. (2010). Judging intoxication. *Behav. Sci. Law*, 29:116–137.
- [Rucci and Casile, 2005] Rucci, M. and Casile, A. (2005). Fixational instability and natural image statistics: Implications for early visual representations. *Netw. Comput. Neural Syst.*, 16(2-3):121–138.
- [Rueden et al., 2017] Rueden, C. T., Schindelin, J., Hiner, M. C., DeZonia, B. E., Walter, A. E., Arena, E. T., and Eliceiri, K. W. (2017). ImageJ2: ImageJ for the next generation of scientific image data. *BMC Bioinformatics*, 18(1).
- [Sadakane et al., 2015] Sadakane, O., Masamizu, Y., Watakabe, A., Terada, S. I., Ohtsuka, M., Takaji, M., Mizukami, H., Ozawa, K., Kawasaki, H., Matsuzaki, M., and Yamamori, T. (2015). Long-Term Two-Photon Calcium Imaging of Neuronal Populations with Subcellular Resolution in Adult Non-human Primates. *Cell Rep.*, 13(9):1989–1999.
- [Samata et al., 2015] Samata, B., Kikuchi, T., Miyawaki, Y., Morizane, A., Mashimo, T., Nakagawa, M., Okita, K., and Takahashi, J. (2015). X-linked severe combined immunodeficiency (X-SCID) rats for xeno-transplantation and behavioral evaluation. *J. Neurosci. Methods*, 243:68–77.
- [San Agustin et al., 2010] San Agustin, J., Skovsgaard, H., Mollenbach, E., Barret, M., Tall, M., Hansen, D. W., and Hansen, J. P. (2010). Evaluation of a low-cost open-source gaze tracker. In *Proc. 2010 Symp. Eye-Tracking Res. Appl. - ETRA '10*, page 77, Austin, Texas.
- [Santaniello et al., 2011a] Santaniello, S., Fiengo, G., Glielmo, L., and Grill, W. M. (2011a). Closed-Loop Control of Deep Brain Stimulation: A Simulation Study. *IEEE Trans. Neural Syst. Rehabil. Eng.*, 19(1):15–24.
- [Santaniello et al., 2011b] Santaniello, S., Fiengo, G., Glielmo, L., and Grill, W. M. (2011b). Closed-loop control of deep brain stimulation: A simulation study. *IEEE Trans. Neural Syst. Rehabil. Eng.*, 19:15–24.

- [Sarem-Aslani and Mullett, 2011] Sarem-Aslani, A. and Mullett, K. (2011). Industrial perspective on deep brain stimulation: history, current state, and future developments. *Front. Integr. Neurosci.*, 5:46.
- [Sato and Maharbiz, 2010] Sato, H. and Maharbiz, M. M. (2010). Recent developments in the remote radio control of insect flight. *Front. Neurosci.*, 4(DEC):199.
- [Sawadsaringkarn et al., 2012] Sawadsaringkarn, Y., Kimura, H., Maezawa, Y., Nakajima, A., Kobayashi, T., Sasagawa, K., Noda, T., Tokuda, T., and Ohta, J. (2012). CMOS on-chip optoelectronic neural interface device with integrated light source for optogenetics. *J. Phys. Conf. Ser.*, 352(1):012004.
- [Schultz et al., 2014] Schultz, S. R., Ince, R. A. A., and Panzeri, S. (2014). Applications of Information Theory to Analysis of Neural Data. *arXiv:1501.01860 [q-bio]*, pages 1–6.
- [Seide and Agarwal, 2016] Seide, F. and Agarwal, A. (2016). Cntk. In *Proc. 22nd ACM SIGKDD Int. Conf. Knowl. Discov. Data Min. - KDD ’16*, pages 2135–2135, New York, New York, USA. ACM Press.
- [Sena et al., 2010] Sena, E. S., Bart van der Worp, H., Bath, P. M., Howells, D. W., and Macleod, M. R. (2010). Publication bias in reports of animal stroke studies leads to major overstatement of efficacy. *PLoS Biol.*, 8(3):e1000344.
- [Sharpee, 2017] Sharpee, T. O. (2017). Optimizing Neural Information Capacity through Discretization. *Neuron*, 94(5):954–960.
- [Sheth et al., 2012] Sheth, S. A., Mian, M. K., Patel, S. R., Asaad, W. F., Williams, Z. M., Dougherty, D. D., Bush, G., and Eskandar, E. N. (2012). Human dorsal anterior cingulate cortex neurons mediate ongoing behavioural adaptation. *Nature*, 488(7410):218–221.
- [Shichida and Matsuyama, 2009] Shichida, Y. and Matsuyama, T. (2009). Evolution of opsins and phototransduction. *Philos. Trans. R. Soc. B Biol. Sci.*, 364(1531):2881–2895.
- [Shoham and Deisseroth, 2010a] Shoham, S. and Deisseroth, K. (2010a). Special issue on optical neural engineering: advances in optical stimulation technology. *J. Neural Eng.*, 7(4):040201.
- [Shoham and Deisseroth, 2010b] Shoham, S. and Deisseroth, K. (2010b). Special issue on optical neural engineering: advances in optical stimulation technology. *J. Neural Eng.*, 7(4):040201.
- [Shu et al., 2009a] Shu, X., Royant, A., Lin, M. Z., Aguilera, T. A., Lev-ram, V., Steinbach, A., and Tsien, R. Y. (2009a). NIH Public Access. *October*, 324(5928):804–807.

- [Shu et al., 2009b] Shu, X., Royant, A., Lin, M. Z., Aguilera, T. A., Lev-Ram, V., Steinbach, P. A., and Tsien, R. Y. (2009b). Mammalian expression of infrared fluorescent proteins engineered from a bacterial phytochrome. *Science (80-.).*, 324(5928):804–807.
- [Siemionow, 2015] Siemionow, M. Z. (2015). *Plastic and reconstructive surgery: Experimental models and research designs*. Springer.
- [Smellie and Robson, 2003] Smellie, W. S. A. and Robson, C. A. (2003). Use of a parallel clinical advisory service to support lipid lowering in primary care. *Qual. Prim. Care*, 11(3):199–203.
- [Sofroniew et al., 2016] Sofroniew, N. J., Flickinger, D., King, J., and Svoboda, K. (2016). A large field of view two-photon mesoscope with subcellular resolution for in vivo imaging. *Elife*, 5:e14472.
- [Song et al., 2017] Song, L., Qian, X., Li, H., and Chen, Y. (2017). PipeLayer: A Pipelined ReRAM-Based Accelerator for Deep Learning. *Proc. - Int. Symp. High-Performance Comput. Archit.*, pages 541–552.
- [Soraghan et al., 2008] Soraghan, C. J., Ward, T. E., Matthews, F., and Markham, C. (2008). Optical safety assessment of a near-infrared brain-computer interface. *IET Irish Signals Syst. Conf. ISSC 2008*, pages 174–179.
- [Sorge and Clarke, 2011] Sorge, R. E. and Clarke, P. B. (2011). Nicotine self-administration. In *Neuromethods*, volume 53 of *Neuromethods*, pages 101–132. Humana Press.
- [Spitler and Gothard, 2008] Spitler, K. M. and Gothard, K. M. (2008). A removable silicone elastomer seal reduces granulation tissue growth and maintains the sterility of recording chambers for primate neurophysiology. *J. Neurosci. Methods*, 169(1):23–26.
- [Stein et al., 2009] Stein, E. W., Maslov, K., and Wang, L. V. (2009). Noninvasive, in vivo imaging of the mouse brain using photoacoustic microscopy. *J. Appl. Phys.*, 105(10).
- [Steinmetz et al., 2017] Steinmetz, N. A., Buetfering, C., Lecoq, J., Lee, C. R., Peters, A. J., Jacobs, E. A. K., Coen, P., Ollerenshaw, D. R., Valley, M. T., de Vries, S. E. J., Garrett, M., Zhuang, J., Groblewski, P. A., Manavi, S., Miles, J., White, C., Lee, E., Griffin, F., Larkin, J. D., Roll, K., Cross, S., Nguyen, T. V., Larsen, R., Pendergraft, J., Daigle, T., Tasic, B., Thompson, C. L., Waters, J., Olsen, S., Margolis, D. J., Zeng, H., Hausser, M., Carandini, M., and Harris, K. D. (2017). Aberrant Cortical Activity in Multiple GCaMP6-Expressing Transgenic Mouse Lines. *Eneuro*, 4(5):ENEURO.0207–17.2017.

- [Stelnicki and Ousterhout, 1997] Stelnicki, E. J. and Ousterhout, D. K. (1997). Hydroxyapatite paste (BoneSource) used as an onlay implant for supraorbital and malar augmentation. *J. Craniofac. Surg.*, 8(5):367–372.
- [Stirman et al., 2014] Stirman, J. N., Smith, I. T., Kudenov, M. W., and Smith, S. L. (2014). Wide field-of-view, twin-region two-photon imaging across extended cortical networks. *bioRxiv*, page 011320.
- [Stockbridge et al., 2012] Stockbridge, C., Lu, Y., Moore, J., Hoffman, S., Paxman, R., Toussaint, K., and Bifano, T. (2012). Focusing through dynamic scattering media. *Opt. Express*, 20(14):15086.
- [Stoma et al., 2011] Stoma, S., Friehlich, M., Gerber, S., and Klipp, E. (2011). STSE: Spatio-Temporal Simulation Environment Dedicated to Biology. *BMC Bioinformatics*, 12:126.
- [Stramaglia et al., 2012] Stramaglia, S., Wu, G. R., Pellicoro, M., and Marinazzo, D. (2012). Expanding the transfer entropy to identify information subgraphs in complex systems. *Proc. Annu. Int. Conf. IEEE Eng. Med. Biol. Soc. EMBS*, 86(6 Pt 2):3668–3671.
- [Sullivan, 2005] Sullivan, M. R. (2005). In Vivo Calcium Imaging of Circuit Activity in Cerebellar Cortex. *J. Neurophysiol.*, 94(2):1636–1644.
- [Takahashi et al., 2006] Takahashi, E., Takano, T., Nomura, Y., Okano, S., Nakajima, O., and Sato, M. (2006). In vivo oxygen imaging using green fluorescent protein. *American Journal of Physiology - Cell Physiology*, 291(4):C781–C787.
- [Tervainen et al., 2005] Tervainen, T., Vauhkonen, M., Kolehmainen, V., and Kaipio, J. P. (2005). Hybrid radiative-transfer-diffusion model for optical tomography. *Appl. Opt.*, 44:876–886.
- [Torres and Frery, 2013] Torres, L. and Frery, A. C. (2013). SAR Image Despeckling Algorithms using Stochastic Distances and Nonlocal Means.
- [Trujillo et al., 2018] Trujillo, C. A., Gao, R., Negraes, P. D., Chaim, I. A., Domissy, A., Vandenberghe, M., Devor, A., Yeo, G. W., Voytek, B., and Muotri, A. R. (2018). Nested oscillatory dynamics in cortical organoids model early human brain network development. *bioRxiv*, page 358622.
- [Uhlhaas and Singer, 2006] Uhlhaas, P. J. and Singer, W. (2006). Neural Synchrony in Brain Disorders: Relevance for Cognitive Dysfunctions and Pathophysiology. *Neuron*, 52(1):155–168.

- [Uneri et al., 2012] Uneri, A., Schafer, S., Mirota, D. J., Nithiananthan, S., Otake, Y., Taylor, R. H., and Siewerdsen, J. H. (2012). TREK: An integrated system architecture for intraoperative cone-beam CT-guided surgery. *Int. J. Comput. Assist. Radiol. Surg.*, 7(1):159–173.
- [U.S. Food and Drug Administration, 2016] U.S. Food and Drug Administration (2016). Listing of CDRH Humanitarian Device Exemptions.
- [Van Dam et al., 2006] Van Dam, R. M., Willett, W. C., Manson, J. A. E., and Hu, F. B. (2006). Coffee, caffeine, and risk of type 2 diabetes: A prospective cohort study in younger and middle-aged U.S. women. *Diabetes Care*, 29:398–403.
- [van Wijk et al., 2015] van Wijk, B. C., Jha, A., Penny, W., and Litvak, V. (2015). Parametric estimation of cross-frequency coupling. *J. Neurosci. Methods*, 243:94–102.
- [Vázquez and Marco, 2012] Vázquez, P.-P. and Marco, J. (2012). Using Normalized Compression Distance for image similarity measurement: an experimental study. *Vis Comput*, 28(11):1063–1084.
- [Viswanathan et al., 2015] Viswanathan, S., Williams, M. E., Bloss, E. B., Stasevich, T. J., Speer, C. M., Nern, A., Pfeiffer, B. D., Hooks, B. M., Li, W. P., English, B. P., Tian, T., Henry, G. L., Macklin, J. J., Patel, R., Gerfen, C. R., Zhuang, X., Wang, Y., Rubin, G. M., and Looger, L. L. (2015). High-performance probes for light and electron microscopy. *Nat. Methods*, 12(6):568–576.
- [von Maltzahn et al., 2011] von Maltzahn, G., Park, J.-H., Lin, K. Y., Singh, N., Schröpke, C., Mesters, R., Berdel, W. E., Ruoslahti, E., Sailor, M. J., and Bhatia, S. N. (2011). Nanoparticles that communicate in vivo to amplify tumour targeting. *Nat. Mater.*, 10(7):545–552.
- [Wählby et al., 2002] Wählby, C., Lindblad, J., Vondrus, M., Bengtsson, E., and Björkesten, L. (2002). Algorithms for Cytoplasm Segmentation of Fluorescence Labelled Cells. *Anal. Cell. Pathol.*, 24(2-3):101–111.
- [Wählby et al., 2004] Wählby, C., Sintorn, I. M., Erlandsson, F., Borgefors, G., and Bengtsson, E. (2004). Combining intensity, edge and shape information for 2D and 3D segmentation of cell nuclei in tissue sections. *J. Microsc.*, 215(1):67–76.
- [Wang et al., 2018] Wang, D. J., Jann, K., Fan, C., Qiao, Y., Zang, Y. F., Lu, H., and Yang, Y. (2018). Neurophysiological basis of multi-scale entropy of brain complexity and its relationship with functional connectivity. *Front. Neurosci.*, 12(MAY):352.

- [Wang et al., 2017] Wang, Y., Riffel, A. T., Owens, J. D., Pan, Y., Davidson, A., Wu, Y., Yang, C., Wang, L., Osama, M., Yuan, C., and Liu, W. (2017). Gunrock. *ACM Trans. Parallel Comput.*, 4(1):1–49.
- [Ward et al., 2018] Ward, L., Dunn, A., Faghaninia, A., Zimmermann, N. E., Bajaj, S., Wang, Q., Montoya, J., Chen, J., Bystrom, K., Dylla, M., Chard, K., Asta, M., Persson, K. A., Snyder, G. J., Foster, I., and Jain, A. (2018). Matminer: An open source toolkit for materials data mining. *Comput. Mater. Sci.*, 152(Nips):60–69.
- [Wei, 2008] Wei, J. T. (2008). Editorial Comment. *J. Urol.*, 180(1):245.
- [Wentz et al., 2011] Wentz, C. T., Bernstein, J. G., Monahan, P., Guerra, A., Rodriguez, A., and Boyden, E. S. (2011). A wirelessly powered and controlled device for optical neural control of freely-behaving animals. *J. Neural Eng.*, 8:46021.
- [White et al., 2013] White, T. P., Gilleen, J., and Shergill, S. S. (2013). Dysregulated but not decreased salience network activity in schizophrenia. *Front. Hum. Neurosci.*, 7:65.
- [Witten et al., 2010] Witten, I. B., Lin, S.-C., Brodsky, M., Prakash, R., Diester, I., Anikeeva, P., Gradinaru, V., Ramakrishnan, C., and Deisseroth, K. (2010). Cholinergic Interneurons Control Local Circuit Activity and Cocaine Conditioning. *Science (80-.).*, 330(6011):1677–1681.
- [Witten et al., 2011] Witten, I. B., Steinberg, E. E., Lee, S. Y., Davidson, T. J., Zalocusky, K. A., Brodsky, M., Yizhar, O., Cho, S. L., Gong, S., Ramakrishnan, C., Stuber, G. D., Tye, K. M., Janak, P. H., and Deisseroth, K. (2011). Recombinase-driver rat lines: Tools, techniques, and optogenetic application to dopamine-mediated reinforcement.
- [Wu et al., 2015] Wu, F., Stark, E., Ku, P. C., Wise, K. D., Buzsáki, G., and Yoon, E. (2015). Monolithically Integrated μ LEDs on Silicon Neural Probes for High-Resolution Optogenetic Studies in Behaving Animals. *Neuron*, 88(6):1136–1148.
- [Xing et al., 2009] Xing, D., Yeh, C.-I., and Shapley, R. M. (2009). Spatial Spread of the Local Field Potential and its Laminar Variation in Visual Cortex. *J. Neurosci.*, 29:11540–11549.
- [Yang et al., 2010] Yang, G., Pan, F., Parkhurst, C. N., Grutzendler, J., and Gan, W. B. (2010). Thinned-skull cranial window technique for long-term imaging of the cortex in live mice. *Nat. Protoc.*, 5(2):213–220.
- [Yoshida et al., 2015] Yoshida, S., Morimoto, Y., Tonooka, T., and Takeuchi, S. (2015). An inhalation anesthetic device for stereotaxic operation on mouse pups. *J. Neurosci. Methods*, 243:63–67.

- [Yoshida Kozai et al., 2012a] Yoshida Kozai, T. D., Langhals, N. B., Patel, P. R., Deng, X., Zhang, H., Smith, K. L., Lahann, J., Kotov, N. A., and Kipke, D. R. (2012a). Ultrasmall implantable composite microelectrodes with bioactive surfaces for chronic neural interfaces. *Nat. Mater.*, 11(12):1065–1073.
- [Yoshida Kozai et al., 2012b] Yoshida Kozai, T. D., Langhals, N. B., Patel, P. R., Deng, X., Zhang, H., Smith, K. L., Lahann, J., Kotov, N. A., and Kipke, D. R. (2012b). Ultrasmall implantable composite microelectrodes with bioactive surfaces for chronic neural interfaces.
- [Young et al., 2015] Young, M. D., Field, J. J., Sheetz, K. E., Bartels, R. A., and Squier, J. (2015). A pragmatic guide to multiphoton microscope design. *Adv. Opt. Photonics*, 7(2):276.
- [Yousif et al., 2008] Yousif, N., Bayford, R., and Liu, X. (2008). The influence of reactivity of the electrode-brain interface on the crossing electric current in therapeutic deep brain stimulation. *Neuroscience*, 156(3):597–606.
- [Yousif and Liu, 2007] Yousif, N. and Liu, X. (2007). Modeling the current distribution across the depth electrode - Brain interface in deep brain stimulation. *Expert Rev. Med. Devices*, 4(5):623–631.
- [Yousif and Liu, 2009] Yousif, N. and Liu, X. (2009). Investigating the depth electrode-brain interface in deep brain stimulation using finite element models with graded complexity in structure and solution. *J. Neurosci. Methods*, 184(1):142–151.
- [Zao et al., 2014] Zao, J. K., Gan, T.-T., You, C.-K., Chung, C.-E., Wang, Y.-T., Rodríguez Márquez, S. J., Mullen, T., Yu, C., Kothe, C., Hsiao, C.-T., Chu, S.-L., Shieh, C.-K., and Jung, T.-P. (2014). Pervasive brain monitoring and data sharing based on multi-tier distributed computing and linked data technology. *Front. Hum. Neurosci.*, 8(June).
- [Zhai et al., 2014] Zhai, R., Zhou, Z., Zhang, W., Sang, S., and Li, P. (2014). Control and navigation system for a fixed-wing unmanned aerial vehicle. *AIP Adv.*, 4(3).
- [Zhang et al., 2010] Zhang, F., Gradinariu, V., Adamantidis, A. R., Durand, R., Airan, R. D., De Lecea, L., and Deisseroth, K. (2010). Optogenetic interrogation of neural circuits: Technology for probing mammalian brain structures. *Nat. Protoc.*, 5(3):439–456.
- [Zhang et al., 2008] Zhang, H. X., Massoubre, D., McKendry, J., Gong, Z., Guilhabert, B., Griffin, C., Gu, E., Jessop, P. E., Girkin, J. M., and Dawson, M. D. (2008). Individually-addressable flip-chip AlInGaN micropixelated light emitting diode arrays with high continuous and nanosecond output power. *Opt. Express*, 16(13):9918.

- [Zhang et al., 2009] Zhang, J., Laiwalla, F., Kim, J. A., Urabe, H., Wagenaar, R. V., Song, Y.-K., Connors, B. W., Zhang, F., Deisseroth, K., Nurmikko, A. V., Van Wagenaar, R., Song, Y.-K., Connors, B. W., Zhang, F., Deisseroth, K., and Nurmikko, A. V. (2009). Integrated device for optical stimulation and spatiotemporal electrical recording of neural activity in light-sensitized brain tissue. *J. Neural Eng.*, 6(5):055007.
- [Zhukova et al., 2009] Zhukova, V., Ipatov, M., and Zhukov, A. (2009). Thin magnetically soft wires for magnetic microsensors. *Sensors*, 9(11):9216–9240.
- [Zhuo et al., 2012] Zhuo, J., Xu, S., Proctor, J. L., Mullins, R. J., Simon, J. Z., Fiskum, G., and Gullapalli, R. P. (2012). Diffusion kurtosis as an in vivo imaging marker for reactive astrogliosis in traumatic brain injury. *Neuroimage*, 59(1):467–477.
- [Zhuo et al., 2016] Zhuo, J.-M., an Tseng, H., Desai, M., Bucklin, M. E., Mohammed, A. I., Robinson, N. T., Boyden, E. S., Rangel, L. M., Jasanoff, A. P., Gritton, H. J., and Han, X. (2016). Young adult born neurons enhance hippocampal dependent performance via influences on bilateral networks. *eLife*, 5.
- [Zimand, 2017] Zimand, M. (2017). Distributed compression through the lens of algorithmic information theory: a primer.
- [Zimmermann et al., 2014] Zimmermann, T., Morrison, J., Hogg, K., and O'Toole, P. (2014). Clearing up the signal: Spectral imaging and linear unmixing in fluorescence microscopy. In *Methods Mol. Biol.*, volume 1075 of *Methods in Molecular Biology*, pages 129–148. Humana Press, New York, NY.
- [Zuluaga-Ramirez et al., 2015] Zuluaga-Ramirez, V., Rom, S., and Persidsky, Y. (2015). Craniula: A cranial window technique for prolonged imaging of brain surface vasculature with simultaneous adjacent intracerebral injection. *Fluids Barriers CNS*, 12(1):24.

Curriculum Vitae

Mark E. Bucklin

6 Front St Chelsea, MA 02150 markbucklin@gmail.com

Education

BOSTON UNIVERSITY,
School of Medicine; Division of Graduate Medical Sciences
Boston, MA
2010-Present

- Currently in 1st year of M.D./Ph.D. program
- Pursuing Ph.D. in Biomedical Engineering

COLUMBIA UNIVERSITY,
Fu Foundation School of Engineering and Applied Science
New York, NY
2005-2009

- B.S. Biomedical Engineering – Biomedical Imaging track
- 3.69 Cumulative GPA
-

MOUNT DESERT ISLAND HIGH SCHOOL
Bar Harbor, ME

2001-2005

Experience

CENTER FOR NEUROBIOLOGY AND BEHAVIOR - CUMC
Technician: Lab of Aniruddha Das, Ph.D.
New York, NY

May 2008-August 2010

- Developed image acquisition software in MATLAB and firmware in embedded C
- Built routines for data management, analysis, visualization, and access over a network
- Constructed a device to measure respiratory patterns in non-human primates
- Upgraded optical imaging system to use optical fibers, enabling simultaneous dual-wavelength intrinsic signal imaging and neural-recording

NORTHEAST HARBOR AMBULANCE SERVICE

EMT/Ambulance Attendant

Northeast Harbor, ME

2005-Present

- Lead care or assist a paramedic
- Completed Intermediate level course for higher level license
- Started IVs, collected blood, and obtained ECGs during >100 hours of clinical rotations

TEACHING AND PROJECTS ABROAD

Medical Volunteer

Nagoda Hospital, Sri Lanka

May-June 2006

- Assisted and observed local medical personnel in rounds and various procedures
- Spent time in General, OB-GYN, Pediatric, Surgical, and Post-Mortem wards

JACKSON LABORATORY

Research Intern

Bar Harbor, ME

2003-2005

- Designed and led study determining the effect of a global growth hormone deficiency on atherosclerosis in mice
- Bred and genotyped mice and performed histology to quantify arterial damage
- Used PCR genotyping to identify QTLs, and taught procedures to incoming students

HANCOCK COUNTY MEDICAL MISSION
Surgeon's Assistant
Ibarra, Ecuador
March 2005

- Directly assisted one general and one vascular surgeon in more than 50 operations
- Provided free-healthcare while gaining valuable medical experience

Skills and Interests

PROGRAMMING: MATLAB, Java, C/C++

INTERESTS: Electronics, Sailing, Traveling, Web Development

References

Aniruddha Das Ph.D., Center for Neurobiology and Behavior, CUMC –
ad2069@columbia.edu

Michael Dennis M.D., St. Mary's Episcopal Church –
newrinkle@aol.com

Heather Frazer, Pd.D., – Frazer@fau.edu